JAEA-Review
2016-026

DOI:10.11484/jaea-review-2016-026

JAEA-Review

# Results and Progress of Fundamental Research on Fission Product Chemistry

## - Progress Report in 2015 -

Masahiko OSAKA, Shuhei MIWA, Kunihisa NAKAJIMA, Fidelma Giulia DI LEMMA
Chikashi SUZUKI, Naoya MIYAHARA, Masaaki KOBATA, Tetsuo OKANE
and Eriko SUZUKI

LWR Key Technology Development Division
Nuclear Science and Engineering Center
Sector of Nuclear Science Research

December 2016

Japan Atomic Energy Agency

日本原子力研究開発機構

国立研究開発法人日本原子力研究開発機構　研究連携成果展開部　研究成果管理課
〒319-1195 茨城県那珂郡東海村大字白方 2 番地4
電話 029-282-6387, Fax 029-282-5920, E-mail:ird-support@jaea.go.jp

Institutional Repository Section,
Intellectual Resources Management and R&D Collaboration Department,
Japan Atomic Energy Agency.
2-4 Shirakata, Tokai-mura, Naka-gun, Ibaraki-ken 319-1195 Japan
Tel +81-29-282-6387, Fax +81-29-282-5920, E-mail:ird-support@jaea.go.jp

JAEA-Review 2016-026

# Results and Progress of Fundamental Research on Fission Product Chemistry
## - Progress Report in 2015 -

Masahiko OSAKA, Shuhei MIWA, Kunihisa NAKAJIMA,
Fidelma Giulia DI LEMMA[*1], Chikashi SUZUKI, Naoya MIYAHARA[※1],
Masaaki KOBATA[※2], Tetsuo OKANE and Eriko SUZUKI

LWR Key Technology Development Division, Nuclear Science and Engineering Center,
Sector of Nuclear Science Research,
Japan Atomic Energy Agency
Tokai-mura, Naka-gun, Ibaraki-ken

(Received November 2, 2016)

A fundamental research program on fission product (FP) chemistry has been conducted since 2012 in order to establish a FP chemistry database in LWR under severe accidents and to improve FP chemical models based on the database. Research outputs are reflected as fundamental knowledge to both the R&D of decommissioning of Fukushima Daiichi Nuclear Power Station (1F) and enhancement of LWR safety. Four research items have thus been established considering the specific issues of 1F and the priority in the source term research area, as follows: effects of boron (B) release kinetics and thermal-hydraulic conditions on FP behavior, cesium (Cs) chemisorption and reactions with structural materials, enlargement of a thermodynamic and thermophysical properties database for FP compounds and development of experimental and analytical techniques for the reproduction of FP behavior and for direct measurement methods of chemical form of FP compounds. In this report, the research results and progress for the year 2015 are described. The main accomplishment was the installation of a reproductive test facility for FP release and transport behavior. Moreover, basic knowledge about the Cs chemisorption behavior was also obtained. In addition to the four research items, a further research item is being considered for deeper interpretation of FP behavior by the analysis of samples outside of the 1F units.

Keywords: Fission Product, Chemistry, BWR, Boron, Reproduction Test, Chemisorption, Outside-1F Unit Samples

---

[※1] Collaborating Engineer
[※2] Senior Post-Doctoral Fellow
[*1] Idaho National Laboratory (Post-Doctoral Fellow until September, 2016)

JAEA-Review 2016-026

# 核分裂生成物化学挙動の解明に向けた基礎研究の成果及び進捗
## ―2015 年度進捗報告―

日本原子力研究開発機構　原子力科学研究部門
原子力基礎工学研究センター　軽水炉基盤技術開発ディビジョン

逢坂　正彦、三輪　周平、中島　邦久、Fidelma Giulia DI LEMMA[*1]、鈴木　知史、
宮原　直哉[※1]、小畠　雅明[※2]、岡根　哲夫、鈴木　恵理子

（2016 年 11 月 2 日　受理）

シビアアクシデント時の軽水炉内の各領域における核分裂生成物（FP）化学に関するデータベースの構築、及びそれらに基づく FP 化学モデルの改良を目的として、2012 年度より FP 化学挙動の解明に向けた基礎研究を開始した。研究成果は福島第一原発（1F）廃炉研究開発及び軽水炉安全性向上のための基礎的知見として反映する。1F 特有の課題やソースターム関連研究における優先度を考慮して、FP 挙動に与えるホウ素（B）放出速度及び熱水力条件の影響、構造材へのセシウム（Cs）化学吸着・反応挙動、FP 化合物の熱力学及び熱物性データベースの拡充、及び FP 挙動再現及び FP 含有化合物の化学形直接測定のための実験・解析技術確立の 4 つの研究項目を設定した。本報告書は、FP 化学挙動の解明に向けた基礎研究の 2015 年の研究成果及び進捗を述べるものである。2015 年の成果として、FP 放出移行挙動再現実験装置の導入を完遂したことが挙げられる。また、Cs 化学吸着に関しての有用な基礎的知見を取得した。4 つの研究項目に加えて、1F 炉外サンプル分析により FP 挙動を評価するための試みについても検討した。

---

原子力科学研究所：〒319-1195 茨城県那珂郡東海村大字白方 2-4
※1　技術開発協力員
※2　任期付研究員
*1　アイダホ国立研究所（2016 年 9 月まで博士研究員）

# Contents

1. Introduction ........ 1
2. Research results and progress in 2015 ........ 2
  2.1 Evaluation of effects of boron release kinetics and thermal-hydraulic conditions on FP chemistry ........ 2
    2.1.1 FP chemical behavior from RPV to RCS regions ........ 2
    2.1.2 Prediction of boron release kinetics from the $B_4C$-SS-Zry mixed melt ........ 4
    2.1.3 Consideration on the effects of chemical reaction kinetics ........ 5
    2.1.4 Synthesis of Cs-containing artificial fuel ........ 6
    2.1.5 Plan for evaluation of FP behavior at PCV region ........ 7
  2.2 Fundamental study on the Cs chemisorption behavior ........ 7
    2.2.1 Basic characteristics of Cs chemisorbed compounds ........ 8
    2.2.2 Ab-initio study on the chemisorbed Cs-Si-Fe-O compounds ........ 8
    2.2.3 Future plan ........ 9
  2.3 Enlargement of a database on thermodynamic and thermophysical properties of FP compounds ........ 9
    2.3.1 Cs-B-O system ........ 10
    2.3.2 Cs-Si-O system ........ 10
  2.4 Development of experimental and analytical techniques for the FP chemistry research ........ 11
    2.4.1 Development of reproduction test technology for FP release and transport ........ 11
    2.4.2 Development of analytical tool incorporating chemical reaction kinetics treatment ........ 12
    2.4.3 Resonance Ionization Mass Spectrometry (RIMS) for direct measurement of chemical form ........ 12
    2.4.4 Hard X-ray Photoelectron Spectroscopy (HAXPES) as a direct evaluation technique of FP chemical states in deposits ........ 12
    2.4.5 TG-DTA-MS apparatus for the direct determination of FP vapor species ........ 13
  2.5 Analysis of samples outside 1F units for the evaluation of FP chemical behavior ........ 14
    2.5.1 Review of research activities regarding environmental sample analysis containing radioactive Cs ........ 14
    2.5.2 Research plan for the analysis of samples outside 1F units ........ 14
    2.5.3 HAXPES development for the measurement of samples outside 1F units ........ 15
3. Concluding summary ........ 16
Acknowledgement ........ 16
References ........ 17

# 目　次

1. 緒言 ........ 1
2. 2015 年度の研究成果及び進捗 ........ 2
  2.1 FP 化学挙動に与えるホウ素放出速度と熱水力条件の影響評価 ........ 2
    2.1.1 RPV から RCS に至る領域における FP 化学挙動 ........ 2
    2.1.2 $B_4C$-SS-Zry 混合溶融体からのホウ素放出速度の予測 ........ 4
    2.1.3 化学反応速度論の影響の検討 ........ 5
    2.1.4 Cs 含有人工燃料の合成 ........ 6
    2.1.5 PCV における FP 挙動評価研究計画 ........ 7
  2.2 Cs 化学吸着についての基礎研究 ........ 7
    2.2.1 Cs 化学吸着化合物の基本的特性 ........ 8
    2.2.2 第一原理計算による化学吸着により生成した Cs-Si-Fe-O 化合物の評価 ........ 8
    2.2.3 今後の研究計画 ........ 9
  2.3 FP 化合物の熱力学及び熱物性データベースの拡充 ........ 9
    2.3.1 Cs-B-O 系 ........ 10
    2.3.2 Cs-Si-O 系 ........ 10
  2.4 FP 化学研究のための実験及び解析技術開発 ........ 11
    2.4.1 FP 放出移行再現実験技術の開発 ........ 11
    2.4.2 化学反応速度論を考慮した解析ツールの開発 ........ 12
    2.4.3 化学形直接測定のための共鳴イオン化質量分析法（RIMS）開発 ........ 12
    2.4.4 沈着物中の FP 化学状態直接評価手法としての硬 X 線光電子分光分析法（HAXPES）開発 ........ 12
    2.4.5 FP 蒸気種直接同定のための TG-DTA-MS 装置開発 ........ 13
  2.5 1F 炉外サンプルの分析による FP 化学挙動評価についての検討 ........ 14
    2.5.1 放射性セシウムを含有する環境試料分析に関わる研究のレビュー ........ 14
    2.5.2 1F 炉外サンプル分析についての研究計画 ........ 14
    2.5.3 1F 炉外サンプル分析のための HAXPES の開発 ........ 15
3. 結言 ........ 16
謝辞 ........ 16
参考文献 ........ 17

## List of Tables

Table 1 Breakdown structure of research ........ 31
Table 2 Changes in formation of B, Cs and I species under a steam-starvation atmosphere due to the decrease in B release from the mixed melt of $B_4C$-SS-Zry ...... 32
Table 3 Calculation results of the changes of Cs chemical species through the RCS to PCV ........ 32
Table 4 Stability evaluation on Cs-Si-Fe-O compounds by ab-initio calculation........ 32

## List of Figures

Fig. 1 Organization for the fundamental research on FP chemistry ........ 21
Fig. 2 Mid-term plan for the fundamental research on FP chemistry ........ 22
Fig. 3 Main framework of the fundamental research on FP chemistry ........ 23
Fig. 4 Reproduction of Cs release rate from MOX fuel in the VERCOR test by the improved CORSOR-M model for MOX fuel ........ 23
Fig. 5 Appearance of prepared FeB sample used in the oxidation and vaporization tests in the B-ReK facility ........ 24
Fig. 6 Schematic view of a small size test facility for FP release and transport ........ 24
Fig. 7 An example of elemental distribution on the surface of SS304 exposed to CsOH vapor ........ 25
Fig. 8 X-ray diffraction patterns of synthesized $Cs_2B_4O_7$ and $CsB_3O_5$ at room temperature ........ 26
Fig. 9 X-ray diffraction patterns of synthesized $Cs_2Si_2O_5$, $Cs_2Si_4O_9$ and $CsFeSiO_4$........ 27
Fig. 10 Appearance of and FP flow in TeRRa facility ........ 28
Fig. 11 HAXPES spectra of Cs 3*d* and I 3*d* core levels for the thermal gradient tube (TGT) samples of (A1) TGT at ~ 650°C, not exposed to $B_2O_3$ vapor, (A2) TGT at ~ 300°C, not exposed to $B_2O_3$ vapor, (B1) TGT at ~ 650°C, exposed to $B_2O_3$ vapor, (B2) TGT at ~ 300°C, exposed to $B_2O_3$ vapor, and (B3) TGT at ~ 150°C, exposed to $B_2O_3$ vapor. Red broken lines are HAXPES spectrum for CsI reference. ........ 29
Fig. 12 Schematic diagram of TG-DTA-MS apparatus ........ 30

# 1. Introduction

A fundamental research program on fission product (FP) chemistry has been conducted in Japan Atomic Energy Agency (JAEA) since 2012 1). The research aims at contributing to both the R&D for decommissioning of Fukushima Daiichi Nuclear Power Station (1F) and the enhancement of LWR safety, by providing basic knowledges of the FP chemistry. FP chemistry has a critical impact on FP release and transport, whose evaluation is a basis for the improved source term assessment under a LWR severe accident (SA). FP chemistry has been recognized worldwide as an important issue for FP related research, and the significance of FP chemistry has also been shown by our comprehensive literature review1). Our review with consideration on the 1F specific conditions has also resulted in adding chemical effects of BWR control rod materials Boron (B) as an important issue1, 2). Thus, the objective of our research is to improve FP chemical models and development of a FP chemistry database for each stage of LWR, i.e. fuel, Reactor Pressure Vessel (RPV), Reactor Cooling System (RCS), Primary Containment Vessel (PCV), Reactor Building (R/B), under a SA mainly based on the experimentally obtained results. Four research items have thus been determined as follows:

(1) Evaluation of effects of B release kinetics and thermal-hydraulic conditions on FP chemical behavior
(2) Clarification of cesium (Cs) chemisorption and reaction behaviors on structural materials at relatively high temperatures such as upper head of RPV
(3) Enlargement of a database on thermodynamic and thermophysical properties of FP compounds formed within a reactor
(4) Development of experimental and analytical techniques for reproduction tests of FP release and transport and of direct measurement methods for chemical form of FP compounds.

The breakdown structure of the research, the research organization and mid-term research plan are shown in Table 1, Fig. 1 and Fig. 2, respectively. They are decided in order to meet the milestones for both the 1F decommissioning R&D and LWR safety enhancement. Main framework of the fundamental research on FP chemistry is shown in Fig. 3. Reproductive tests by the TeRRa facility (Test bench for FP Release and tRansport), whose details are described in 2.4.1, and chemical reaction kinetic analysis of TeRRa test results are centered in developing the database and improved models for FP chemistry. In addition, separate effect tests such as Cs chemisorption and B release kinetics are also performed for detailed mechanistic analysis of the fundamental phenomena. The models and database obtained will then be finally validated by hot tests using a real irradiated fuel sample. This will certify the use of models and database in SA analysis codes and will provide fundamental information for the 1F decommissioning R&D.

This report describes results and progress of the fundamental research on FP chemistry for the year 2015, following the last progress report[3)]. Besides, the plan for a new research item focused on the analysis of samples outside 1F units is also described. This will be used to infer FP chemical behavior inside 1F. Such backward-type analysis could also be useful for the enhancement of in-reactor SA progression evaluation, on the conditions that they will be appropriately combined with the forward-type analysis results obtained by SA codes.

## 2. Research results and progress in 2015

### 2.1 Evaluation of effects of boron release kinetics and thermal-hydraulic conditions on FP chemistry

The 1F-SA has recalled the importance of chemical effects of $B_4C$ control blade material in BWR and of the atmosphere during a SA on FP chemistry. Relatively less knowledge has been obtained so far for the chemical effects of $B_4C$ control blade material compared with those of the Silver (Ag)-Indium (In)-Cadmium (Cd) used in the control rod of PWR. Indeed B species could be released under a BWR SA from a mixed melts consisted of the control blade materials, $B_4C$-stainless steel (SS)-Zircaloy (Zry). However the knowledge on the B release behavior from the mixed melts is only qualitative[4)]. Previous thermodynamic studies have shown that the presence of B can have a significant impact on the chemistry of Cs and Iodine (I) by forming a stable compound, $CsBO_2$[5)]. In addition, the representative FP release and transport experiment Phebus-FPT3, which incorporated a $B_4C$ control rod in the experimental system[6)], has given rise to some enigmatic results such as enlarged gas I fraction in the PCV. These results are believed to be due to the existence of $B_4C$ control rod under certain atmospheres. In order to comprehensively understand the effects of $B_4C$ and atmosphere on FP chemistry, we perform a fundamental study for the effects of B release kinetics and thermal-hydraulic conditions on FP chemistry. The obtained data and knowledge by the experiments were then analyzed considering chemical reaction kinetics as described in section 2.4.2 to construct the FP chemistry database.

### 2.1.1 FP chemical behavior from RPV to RCS regions

The FP chemical behavior from RPV to RCS regions was investigated by both experimental and analytical means to evaluate the effects of B release kinetics and atmosphere.

(1) Effects of B release kinetics on the Cs and I vapor species[7)]

Effects of B release kinetics on the Cs and I vapor species were investigated by a combined calculation of elemental release rate from fuel and chemical equilibrium.

Formation of stable Fe-B compounds in the $B_4C$-SS-Zry mixed melt was assumed to suppress vaporization and release of B. Atmospheric dependences of the release kinetics for Cs, I, Mo, C and B were considered in the elemental release calculation by using several CORSOR models with atmospheric dependent parameter sets. Results showed that the B release was enhanced above approximately 2,250 K, where $CsBO_2$ and high volatile atomic I became the major vapor species under a steam atmosphere. On the other hand, the formation of $CsBO_2$ was suppressed under a steam-starvation atmosphere due to much lower B release caused by the formation of stable Fe-B compounds. This resulted in a lesser formation of gaseous hydrogen iodide, HI, and the high volatile atomic I, as shown in Table 2. These prediction results finally showed that B release kinetics, as well as the atmosphere, played an important role for the fractions of formation of Cs and I vapor species.

### (2) Effects of atmosphere on the release behavior of non γ-emitting elements[8)]

There are not plenty of data for release behaviors of semi- or low-volatile non γ-emitting elements, such as Sr, U, in spite of their potential importance on the radiological consequences of a SA. One reason for this shortage of data is related to the difficulty of obtaining systematic experimental data, since the destructive chemical analysis is needed which requires great effort compared with nondestructive γ-spectrometry applicable to γ-emitting nuclides. A collaborative work among JRC-Karlsruhe, CEA and JAEA has thus been conducted to evaluate the release and transport behavior of non γ-emitting nuclides by using the chemical analysis data set obtained from deposits in VERCORS HT2 (steam atmosphere, $UO_2$) and HT3 (hydrogen atmosphere, $UO_2$) tests. The focusing point was the atmospheric dependence on the release behavior, as these FP (semi- or low-volatile non γ-emitting elements) could become volatile due to atmosphere alteration. These experimental results could provide important information to improve the database for FP and actinide release. A new finding was obtained for Rb, Sr and U release behavior; Rb could behave similarly to Cs, while Sr and U were revealed to have notably high release rates under hydrogen and steam atmospheres, respectively. Experimental information on the release behaviors of Tc and Pd was also obtained, which were used to improve the database.

### (3) Effects of MOX fuel on the FP and actinides release behavior

Although it is pointed out that the Cs release behavior from MOX fuel differs from that from $UO_2$ fuel, there are no specific models that can depict the Cs release kinetics from MOX fuel. Construction of such model has thus been carried out based on the CORSOR-M model[9)]. The available, although limited, quantitative experimental data for Cs release from MOX fuels were reviewed to determine the parameter sets for the CORSOR-M model. From the results of the VERCORS test[10)], a different Cs release behavior of MOX fuel from that of $UO_2$ fuel was reported. This was attributed to the specific heterogeneous microstructure of the MOX fuel that contains the locally high burnup Pu spots. On the other hand, the difference in the Cs release behavior of MOX fuel from that of $UO_2$ fuel in VEGA test 11) has been reported to be caused by a high fuel linear power. In both cases, nevertheless, MOX fuel would have enhanced the Cs release at lower temperature region. Thus a parameter set for the CORSOR-M for the Cs release from the MOX fuel has been obtained by regression analyses of the experimentally obtained Cs release rate. So obtained improved CORSOR-M model for the MOX fuel was found to reproduce well Cs release behavior in the VERCORS test especially at lower temperature region, as shown in Fig. 4.

As for the release behavior of non $\gamma$-emitting nuclides from MOX fuel, that under reducing atmosphere was also investigated by the analysis of VERCOR RT7 results8). This showed that the effects of MOX fuel on the FP and actinide release behaviors have a small impact compared with those of atmosphere and high burnup of fuel.

### 2.1.2 Prediction of boron release kinetics from the $B_4C$-SS-Zry mixed melt

Current models implemented in SA codes have been unsuccessful in simulating detailed core degradation in real and simulated SAs4). This has been partially related to crude models for $B_4C$-SS-Zry mixed melts behavior. Such melts can be formed by the interaction of the BWR control blade material $B_4C$ with cladding and structural materials during a SA. Their formation can affect strongly the B release kinetics and consequently the FP behavior7). Thus the improvement of the material properties database for $B_4C$-SS-Zry mixed melts has been carried out, as this is needed to obtain better predictions in SA and finally for a better understanding of the effect of B on FP behavior. Our experiments aim at providing thermodynamic and kinetic models of the oxidation and B release kinetic for these complex melts. Separate effect tests were thus performed with the "B-ReK" (Boron Release Kinetics) facility. The B-ReK consists of a Thermogravimeter - Differential Thermal Analyzer (TG-DTA) connected to a customized steam generator controlling the oxygen partial pressure by the $H_2O/H_2$ equilibria. The B-ReK enables us to monitor sample oxidation and vaporization kinetics as functions of not only temperature but also oxygen potential. Samples are heated in the TG-DTA to high temperatures. To evaluate B release kinetics from these complex melts, we have first analyzed the behavior of the simple binary compound4), such as the one related to $B_4C$-Fe (FeB, $Fe_2B$), and $B_4C$-Zry ($Zr_2B$) interactions. The appearance of the prepared and post-tested samples is shown in Fig. 5. The oxidation and vaporization study on the $B_4C$-Fe compounds is now underway. From the first test we observed that the oxidation kinetics has a relation with the Fe to B ratio in the sample compound. This ratio influenced the vaporization kinetics as it governs the formation behavior of the different oxide compounds (Fe-B-O vs Fe-O)[12]. In the future, more complex phases will be analyzed, as the one generated by $B_4C$-SS interaction (e.g. $(Fe_{0.75}Cr_{0.1}Ni_{0.08})_2B$, $(Fe_{0.47}Cr_{0.51}Ni_{0.02})B$ [13]). The $B_4C$-SS-Zry mixed melts with the compositions corresponding to actual SAs will finally be tested in order to obtain quantitative data on B release kinetics from the $B_4C$-SS-Zry mixed melts.

### 2.1.3 Consideration on the effects of chemical reaction kinetics

For the evaluation of FP chemistry at intermediate temperature region such as in the RCS, chemical reaction kinetics effects should be considered[14]. We have thus determined a mid-term plan, which aims at constructing a combined methodology of experimental and analytical means for considering chemical reaction kinetics. The experimental part mainly consists of reproduction tests of FP release and transport using the TeRRa facility (see 2.4.1), while the analytical methodology will be developed based on a tool implementing chemical reaction kinetics. Preliminary works are mentioned in this sub-section, focused on the prediction of FP chemical forms in RCS region using a constant reaction rate. The experimental data acquisition using a small test facility for FP transport behavior is also described.

(1) Prediction of FP chemical forms in RCS and PCV using constant reaction rates[15]

FP chemical forms under the conditions experienced in the RCS and PCV (from 1,000 K to 400 K) regions of the VERCORS HT2 (steam atmosphere) and HT3 (hydrogen atmosphere) tests were predicted by a simple method, considering predetermined chemical reactions with a constant chemical reaction rate regardless of temperature. A Cs-I-Mo-Te-B-O-H system was assumed for these tests. Determination of dominant chemical reactions in each test were made, referring to results of chemical equilibrium calculations at each position of the test loop under the atmosphere of each test using the elemental inventory in the samples used for the tests. The constant chemical reaction rate for the predetermined chemical reaction was then determined so that the calculation results for the deposited elemental amounts agreed with those obtained by the experiment. It was assumed in the calculation that vapor species condense and deposit when the vapor pressures of the species became higher than their saturated vapor pressures at each position. Calculation results for Cs vapor species through the RCS to PCV is shown in Table 3. It was found that the major chemical species presented under the steam atmosphere were CsOH, $Cs_2MoO_4$ and $CsBO_2$, while Cs, CsI, $CsBO_2$ and $Cs_2Te$ were observed under the hydrogen atmosphere. It is seen under the steam atmosphere that Cs was deposited as $Cs_2MoO_4$ and $CsBO_2$ in the higher temperature region (> 800 K), while unreacted CsOH was transported and deposited in the lower temperatures region (< 800 K). On the other hand, under the hydrogen atmosphere, Cs was deposited as $Cs_2Te$ and $CsBO_2$ in the higher temperature region (> 800 K), while CsI and Cs were transported and deposited in the lower temperature region (< 800 K). Although this method is simple and rather crude as it assumes only dominant chemical reactions and constant reaction rates, the trend of Cs chemical species could be speculated from the experimentally obtained elemental distribution in the deposits.

(2) Experimental data acquisition of chemical reaction under RCS and PCV conditions 16)

Chemical behaviors of FP and B in gas phase have been investigated mainly in European institutes 17), although still a certain degree of uncertainty remains. On the other hand, there is no data on a solid-gas phase chemistry for FP and B. A preliminary test using a small-size test facility, as shown in Fig. 6, has been carried out in order to obtain first basic data for the solid-gas phase FP - B chemical reactions. This test is conducted under a contract with the Nuclear Regulation Authority of Japan. The reaction of $B_2O_3$ vapor/aerosol with Cs and I deposits was investigated under a reductive atmosphere. A CsI powder was heated up to its total vaporization and then deposited on SS thermal gradient tubes (TGT) having a linear temperature gradient, from 1,023 K to 423 K. Results showed that the deposition occurred mainly in the TGT region from 770 K to 670 K. The X-ray Diffraction Analysis (XRD) and Inductively Coupled Plasma - Mass Spectrometry (ICP-MS) on the deposits showed that the chemical form was the same as that of the sample powder, namely CsI. The vaporization and reaction of $B_2O_3$ with deposits was then carried out. The ICP-MS analysis on the deposits exposed to the $B_2O_3$ vapor/aerosol showed that only I amount in the deposits decreased by approximately 30 % compared with that of Cs amount. Raman spectroscopy on the deposits showed the formation of Cs-B-O compounds. These results imply that a significant amount of I was vaporized as a volatile form due to the formation of Cs-B-O compounds. It is concluded that the B vapor species could significantly affect the chemical behavior of Cs and I by a solid-gas phase reaction.

### 2.1.4 Synthesis of Cs-containing artificial fuel

A systematic investigation on the release and transport behavior of volatile elements finally requires real irradiated fuels to be used in tests. However, since such systematic tests with many irradiated fuels are unrealistic, an artificial fuel sample (SIMFUEL) containing volatile FP elements could be a promising alteration. A challenge for a synthesis of SIMFUEL containing Cs, which is easily vaporized during heat treatment, has started as a collaborative work with Osaka University and Fukui University. The synthesis was performed by the spark plasma sintering (SPS) method. The SPS can greatly lower the sintering temperature and time compared to other sintering methods as demonstrated by

ITU[18], which can suppress the vaporization loss of Cs during sintering. The first test was carried out with $CeO_2$ as a surrogate of $UO_2$[19]. The characterization of sintered samples showed that CsI was successfully incorporated in the $CeO_2$ matrix having a relatively high density. TEM observation will be carried out in near future on the SPS sintered samples to further investigate the physical/chemical state of CsI in the sample.

### 2.1.5 Plan for evaluation of FP behavior at PCV region

A fundamental study is now being considered for the evaluation of FP behavior at PCV region. Such FP-related study at PCV is of crucial importance since PCV is actually the final boundary to the environment. As all the FPs exist as an aerosol form at PCV except for a small amount of gaseous FPs such as Kr, Xe, gaseous I and Ru, the main body of the study is regarding to the aerosol behavior. Various aerosol properties, morphology, chemical composition, water solubility, etc., will be investigated as functions of chemical conditions experienced in the reactor by using the TeRRa and other facilities. The characterization results can contribute to both the 1F decommissioning R&D and LWR safety enhancement. An example for the former is as input data for the evaluation of samples outside 1F units, as described in section 2.5. On the other hand, we are now planning to perform a fundamental study towards establishment of analytical methodology based on mechanistic models for the venturi scrubber system that is employed in Japanese NPPs as the filtered venting system. As crude models are adopted in SA codes for the filtered venting, it is difficult for the constructor to make the best estimate analysis of FP release to the environment at a SA. Results of characterization and decontamination tests by a simulated filtered venting system device can be useful for the construction of such mechanistic model.

## 2.2 Fundamental study on the Cs chemisorption behavior

Chemisorption is of importance during a SA, as it can influence FP retention in the RPV and thus the amount of radioactive materials released to the environment. However shortage of knowledge and data for the chemisorption make construction of detailed models difficult. Previous studies showed only a limited description of such deposits[20]. The detailed model that incorporates chemical process of the chemisorption behavior is believed to be required for the effective prediction of Cs deposits in 1F. We have therefore performed fundamental studies for a deep understanding of this phenomena and its modelling for SA codes. Moreover, as information on the distribution, composition and properties of such chemisorbed deposits can have significant impact on the decommissioning of reactor, they could also be useful for the 1F decommissioning practice.

### 2.2.1 Basic characteristics of Cs chemisorbed compounds

Focus of our experimental studies for CsOH chemisorption is placed on the difference of several kinds of SS samples used as simulants of reactor structural materials. A series of chemisorption tests have been carried out under conditions simulating a BWR SA, i.e. 1,073 K to 1,273 K under Ar-5%$H_2O$-5%$H_2$ atmosphere on two types of SS, namely type 304 (SS304) and 316 (SS316). As the SS316 contains several percent of Mo, it was used to investigate the effects of Mo on the Cs chemisorption behavior. Results were analyzed and interpreted with the support of chemical equilibrium calculations. The Cs deposits onto SS samples were analyzed after the chemisorption tests by various analytical techniques (Scanning Electron Microscope /Energy Dispersive X-ray spectroscopy (SEM/EDX), Raman spectroscopy, XRD, ICP-MS) for the characterization of deposited compounds. Results showed the importance of the presence of reactive minor compounds in SS such as Si, Mo, which can influence the chemical form of the deposit compounds and their amount. An example of elemental distribution on the surface of SS304 exposed to CsOH vapor is shown in Fig. 7 21). The chemisorbed compound was revealed to be $CsFeSiO_4$ for both SS304 and SS316 samples. The amount of this chemisorbed compound was in relation with Si content in the SS sample. Namely, the higher Si content in SS was, the higher the Cs chemisorbed amount was. Besides, a small amount of Cs-Mo-O compounds were observed on the SS316 sample surfaces. The $CsFeSiO_4$ compound was observed not only on the sample surface but also in the depth of the sample. Finally we investigated the re-vaporization behavior of these chemisorbed compounds, which resulted in the greater stability of $CsFeSiO_4$ than that of Cs-Mo-O compounds.

### 2.2.2 Ab-initio study on the chemisorbed Cs-Si-Fe-O compounds

For the clarification of Cs chemisorbed compounds observed in our experiment, an ab-initio evaluation on the stability of Cs chemisorbed compounds was carried out. While $CsSiFeO_4$ being the Si to Cs ratio of 1 was identified by XRD on the surface of tested sample, the similar experiment conducted previously in SNL have suggested the formation of Cs-Si-O compounds having the Si to Cs ratio of 2 from the elemental distribution analysis by EPMA. The present ab-initio study aims at identifying the likely Cs chemisorbed compounds formed on the SS surface based on the evaluation of the stability of compounds. This evaluation was made by comparing the difference of energy of Cs-Si-Fe-O compounds with that of the reference compound. Each component metal oxide was set as the reference compounds, specifically, $Cs_2O$, $4SiO_2$ and $Fe_2O_3$. Within the predetermined numbers of each elements (Cs, Si, Fe and O), ab-initio calculations on systems consisted of realistically existing compounds were carried out by using VASP code 22). The calculation results showed that $Cs_2Si_4O_9$ and $CsSi_2FeO_6$ were the most stable compounds among the Cs-Si-O and Cs-Si-Fe-O compounds, respectively, as shown in Table 4. Higher stability of Cs-Si-Fe-O compounds than that of Cs-Si-O is of note, which is consistent with our experimental results. The most stable compound for Cs-Si-Fe-O was computed to be $CsSi_2FeO_6$, while that actually observed in our experiment was $CsSiFeO_4$. In the present calculations, conditions were within the adiabatic approximation for the bulk state. In addition, $CsSiFeO_4$ was formed on the SS surface in the experiment, where richer Cs is expected to be available from gas phase than inside the SS matrix. These could be reasons for the difference of resultant stable compounds between the calculation and experiment. This difference will be investigated further.

### 2.2.3 Future plan

Our following studies will concentrate on the effect of atmosphere and other FPs and released materials (e.g. B, etc.) during a SA on the chemisorption mechanism, towards the establishment of improved model. A chemical equilibrium analysis is now underway for the chemical effects of Mo and B on the Cs chemisorption. A two-step reaction for the Cs chemisorption onto SS is assumed and being investigated, taking into account the effects of $Cr_2O_3$ layer formed onto the SS surface and of the duplex oxide layers (i.e. $Fe_3O_4$ outer layer and $Fe_2CrO_4$ inner layer). A basic study on the Si behavior in the oxide layer is also underway as a collaborative work with Tohoku University. The investigations on the mechanical and thermos-physical properties of Cs chemisorbed deposits are also being considered, as they are important properties for the 1F decommissioning practice.

A topical issue is a TEM study on the Cs-chemisorbed SS surface. It can contribute to elaborate a process model, which is the final goal of our chemisorption studies. In the assumed two-step reaction, the Cs chemisorption reaction is initiated by Cs reaction with outer $Cr_2O_3$ layer to form Cs-Cr-O compound, followed by the reaction with Si coming from inner part of SS by the diffusion to the surface via grain boundary. The TEM analyses are expected to help observe these process, for instance, Si migration behavior, nano-scale distribution of different Cs chemisorbed compounds, residual Cs-Cr-O phase, etc. In particular, TEM analyses are expected to reveal the existence of Cs-Si-Fe-O having different chemical compositions, as shown by the experiment and the ab-initio calculation, namely $CsSiFeO_4$ and $CsSi_2FeO_6$.

## 2.3 Enlargement of a database on thermodynamic and thermophysical properties of FP compounds

Cesium forms various kinds of compounds in the reactor under a SA due to its active chemical affinity to other elements. Thermodynamic evaluation plays an important role in the evaluation of FP chemistry, e.g. a preliminary prediction of chemical species formed, interpretation of chemical analysis results and so on. We have thus preparing thermodynamic database mainly for the Cs compounds by means of high temperature mass spectrometry.

### 2.3.1 Cs-B-O system

In a BWR SA, as a large amount of B is used as neutron absorber material, cesium metaborate, $CsBO_2$, is predicted to be formed as the main chemical form of cesium compound[5]. On the other hand, according to Girault and Payot[23] who investigated B effects on FP transport and deposition behaviors in the Phebus FPT tests, the thermodynamic calculations show only a limited impact of B on Cs chemistry. This disagreement might be resulted from a lack of thermodynamic data for various cesium borates. Thermodynamic properties are only available for $CsBO_2$, although many other ternary compounds exist such as $Cs_2B_4O_7$ and $CsB_3O_5$. Therefore, we have started to clarify the thermodynamic properties of the cesium borates, especially those of $CsB_3O_5$, which has the highest melting temperature and is therefore expected to be the most thermodynamically stable among the cesium borates. In order to experimentally obtain such thermodynamic data, information on the phase relations at high temperatures is necessary. However, the phase diagrams reported in the past do not agree with each other[24, 25]. We have thus further investigated the phase relations in the region of $2 \leq B_2O_3/Cs_2O \leq 3$ using a powder XRD and TG-DTA. From our analyses we observed that two phases exist at room temperature, $Cs_2B_4O_7$ and $CsB_3O_5$, while no $Cs_3B_7O_{12}$ was found as shown in Fig. 8. The last phase was previously reported to be present as one of the largest structures known in an anhydrous inorganic material[26]. Further, TG-DTA curves suggested existence of a high temperature phase which was previously indicated in phase diagrams[24]. This phase might be $Cs_3B_7O_{12}$ because a similar compound of $Rb_3B_7O_{12}$ has been observed at similar temperature ranges by high temperature XRD[27]. We have a plan to check further such a high temperature phase by using XRD.

### 2.3.2 Cs-Si-O system

The formation of $CsFeSiO_4$ in the Cs chemisorbed deposit was found in our experiment as already mentioned in 2.2.1. However, only a few thermodynamic and thermophysical properties of cesium silicates[28] and only crystal structure data of $CsFeSiO_4$[29] have been reported in the past. Therefore, we have prepared these compounds to experimentally clarify their thermodynamic and thermophysical properties. Fig. 9 shows the XRD patterns of cesium silicates prepared in this study. The samples were prepared by powder metallurgical techniques. Both $Cs_2Si_2O_5$ and $Cs_2Si_4O_9$ were synthesized at 1,123 K in air, while $CsFeSiO_4$ was synthesized at 1,073 K. As shown in this figure, the samples of $Cs_2Si_2O_5$, $Cs_2Si_4O_9$ and $CsFeSiO_4$ seem to be successfully prepared. The prepared samples will be used in the future not only for the investigation of the thermodynamic and thermophysical properties but also as standard samples for e.g. hard X-ray photoelectron spectroscopy study (see 2.4.4).

## 2.4 Development of experimental and analytical techniques for the FP chemistry research

The key issue for the FP chemistry research is direct experimental evaluation of the FP chemical species. Reproduction techniques for the FP release and transport behavior under well-characterized multi-physics conditions are another important subject to be developed. Moreover, also a tool for analysis of experimentally obtained FP chemistry related data is also needed with taking chemical reaction kinetics into consideration. In this section, the present status and plan for the development of these techniques are described.

### 2.4.1 Development of reproduction test technology for FP release and transport

A test facility for the reproduction of FP release and transport under a SA condition is being developed. The name of the test facility is TeRRa (Test bench for FP Release and tRansport). The TeRRa has a simple path of a straight pipe for FP migration in order to minimize the thermal-hydraulic influences. Fig. 10 shows the appearance of and FP flow in the TeRRa facility. In the TeRRa facility, simulated fuels containing FP and/or structural material elements can be heated by a high frequency induction furnace up to 2,500 K with/without steam injection. The evaporated FPs are then transported from the induction furnace part to the TGT part having linear temperature gradient from 1,000 K to 400 K along the downstream. Airborne aerosols can be extracted at each 100 K of the temperature range of the TGT, and they are then trapped by a cascade impactor for the evaluation of the particle size distribution. Aerosol size distribution can also be measured by an on-line aerosol spectrometer equipped at the upstream of impactor, which can give mutually compensative information on the aerosol formation and growth. Small coupons made of various materials are also set in desired parts in the tube, which can collect the FP deposits and/or chemically absorbed FP compounds. These trapped and deposited samples can be then subjected to off-line analyses by SEM-EDX, XRD, Raman spectroscopy, X-ray Photoelectron Spectroscopy (XPS), and so on. These analyses give essential information about the FP chemistry at different temperatures and chemical conditions, which can help us identify the main chemical reactions occurred under the RCS or PCV conditions. Although a part of the TeRRa design referred to the CHIP facility in IRSN30), usage of solid samples in the higher temperature up to fuel melting and the on-line aerosol size measurements are unique characteristics of the TeRRa.

The first performance test of the TeRRa will be conducted using a simple compound sample such as CsI. This test is expected to show that the TeRRa can control the temperature condition from fuel to PCV as expected and reproduce basic FP release and transport behavior such as chemical reaction, aerosol growth and deposition. Further reproduction tests using simulated fuels containing representative elements such as Cs, I, B will be conducted to acquire basic data for FP chemistry and aerosol size distribution for B containing system.

### 2.4.2 Development of analytical tool incorporating chemical reaction kinetics treatment

As mentioned in sub-section 2.1.3, it was revealed that FP mass balance could precisely be evaluated by considering chemical reaction kinetics. This clearly indicates the necessity of chemical reaction kinetics when analyzing experimental results of reproduction tests. The development of an analytical tool incorporating chemical reaction kinetics has therefore started. The tool is based on a commercial computational fluid dynamics code "ANSYS-FLUENT" 31). The ANSYS-FLUENT code can simulate fluid dynamics in 3-D geometry, incorporating treatments for chemical reaction kinetics and aerosol growth. An important issue is to have a reliable database for the chemical reaction rate constants for all the possible reactions. Some data will be derived from literatures, and the remained will be estimated by ab-initio calculations for the gaseous phase reactions in the database. The prepared dataset will then be used to screen all chemical reactions and excluding practically unrealistic ones using the CHEMKIN code 32) in a 1-D steady-state plug flow condition.

### 2.4.3 Resonance Ionization Mass Spectrometry (RIMS) for direct measurement of chemical form

A quick on-line analysis system for FP chemical form is being developed based on Resonance Ionization Mass Spectrometry (RIMS). A basic study for the detection of Cs-I-B compounds in deposits has been carried out 33). Lasers for selective resonance ionization of I and B have been elaborated by combining and optimizing various kinds of original lasers. Performance tests showed that the RIMS could directly detect the chemical form of CsI or $CsBO_2$. Although further development is needed for the construction of an on-line measurement system for FP species in gas phase, it can be said that the RIMS technique can be a promising candidate as an applicable technique to the analysis of Cs chemical form in the FP deposits.

### 2.4.4 Hard X-ray Photoelectron Spectroscopy (HAXPES) as a direct evaluation technique of FP chemical states in deposits

HAXPES, which uses the X-rays with photon energy of typically above 5 keV, is significantly more bulk-sensitive than conventional photoelectron spectroscopy (PES) using photon energy of vacuum-ultra-violet (VUV) or soft-X-ray (SX) regions. Therefore, HAXPES has an advantage that measurements without surface cleaning process are capable, while the surface cleaning process is inevitable for conventional PES in VUV or SX regions because their spectra should be strongly dominated by outermost surface layers that should be heavily contaminated by oxygen and carbon. In addition, HAXPES would be useful to observe the signal of heavy elements such as Cs and I in the valence band spectra composed of complex electronic structures. To understand the transport behavior of CsI in a reproduction heating test simulating a BWR SA, we have investigated the temperature dependent chemical forms of Cs/I products on the surface of Ni-made TGT and chemical effects of $B_2O_3$ vapor on them by means of HAXPES 34). As demonstrated in Fig. 11, the deposition in the chemical form of CsI was dominant in the temperature range below ~ 300 °C in the absence of reaction with $B_2O_3$, while Cs was deposited in a different chemical form without I on the surface at higher temperature around 650°C. On the other hand, in the case that the surface was exposed to $B_2O_3$ vapor, noticeable CsI-decomposing chemical reaction was observed for the case at specific temperature range around 300°C. The result suggests a following scenario: while CsI deposited on the surface of reactor body structures would be stable at relatively low temperatures, an exposure to B vapor on the structure surface might induce revaporization of Cs through decomposition of CsI.

### 2.4.5 TG-DTA-MS apparatus for the direct determination of FP vapor species

A combined apparatus consisting of a TG-DTA coupled with a quadrupole mass spectrometry (MS), TG-DTA-MS, has been considered useful to determine FP vapor species just after their release from fuel. As a commercial TG-DTA-MS apparatus is guaranteed only for the determination of gas species, no explicit capability is given for the detection of volatile condensable species like CsOH and CsI. The volatile condensable species are considered to condense and deposit especially at the interface between TG-DTA and MS parts. Development of this technique therefore focuses on improvement of this interface, the skimmer interface as schematically shown in Fig. 12, so that vapor species generated in the TG-DTA part can be introduced into the MS part smoothly without condensation. Many trial tests in order to optimize the geometry and various conditions such as flow rate, flow path, ionization mode and voltage, etc. have been carried out using CsI as test samples 35). At the present, atomic I generated by the fragmentation of CsI could be detected. Further challenge is required to achieve the detection of Cs vapor species such as CsI, CsOH, $Cs_2MoO_4$, which are believed to be representative of Cs vapor species released from fuel. As another utilization of this device would be for the evaluation of FP gas release behavior, since the important gaseous species $I_2$, as well as FP gas of He, Kr, Xe, could be measured by this device.

## 2.5 Analysis of samples outside 1F units for the evaluation of FP chemical behavior

### 2.5.1 Review of research activities regarding environmental sample analysis containing radioactive Cs

Cs-bearing spherical particles in the environment surrounding the 1F were first found by Adachi et al.36) and characterized by Y. Abe et al.37). They found that radioactive Cs was included together with several metal elements such as Fe, Zn and Mo with a high oxidation state. The size of the particles was of about several μm. Following their findings, Satou et al.38) have carried out more systematic analyses, trying to elucidate the origin of the particles. They found that there were two types of particles having different diameters, one of several μm and others of several-hundred μm, respectively. A combined synchrotron radiation X-ray analyses have shown that Mo, Te, Sb, Ag etc. were included as well as the radioactive Cs in a silica-glass matrix. Since the two types of particles having different diameters showed different radioactivity ratios of $^{137}$Cs to $^{134}$Cs, they were found to be originated from 1F unit 1 and 2, respectively. The ratio is known to have unique values to each unit caused by different fuel specifications. Other Cs-bearing micro particles were collected and analyzed by Yamaguchi et al.39). Their particles having diameter of 2μm showed concentration gradient for Cs that increased from center to surface in the silica-glass matrix.

### 2.5.2 Research plan for the analysis of samples outside 1F units

As mentioned in the previous sub-section, the samples outside 1F units could have given some interesting indication for the origin of the radioactivity released to the environment. On the other hand, many environmental radioactive waste samples have been analyzed, such as rubbles, contaminated water and so on, in order to characterize the distribution of radioactive inventory for the future treatment and disposal40). A few samples taken from 1F R/B have also been analyzed for the purpose of grasping the contamination situation41). However, although a large number of sample have been analyzed as a total, no systematic database has been created as each analysis was carried out for the different purposes. In addition, only the elemental analyses have been made so far for the waste samples that account for the most part of the available data of environmental samples. Detailed synchrotron radiation X-ray analyses for the purpose of investigating the chemical state of the contained elements have only been performed on few Cs-bearing particles. More detailed information about not only the elemental analysis but also various information such as chemical state is therefore required to grasp the in-reactor FP behavior. In particular, the FP chemical state in the samples outside 1F units would be of value, since this information could be used to infer FP chemical behavior inside 1F by backward-type analysis and to, in some degree, understand the SA progression.

We are now considering performing a systematic analysis of various samples collected outside the 1F units in order to obtain the FP chemical state in the sample. One candidate for such analysis is the Hard X-ray Photoelectron Spectroscopy (HAXPES). The HAXPES has indeed been successfully applied to the FP deposit sample analysis34). The advantage of HAXPES is that the sample surface preparation for the measurement can be omitted, thanks to the capability of attainment of the X-ray into deeper area of the sample around several tenths of nm. This is an advantage of the HAXPES, which permits to perform a large number of analyses in shorter time and therefore is expected to make a reliable systematic study to understand in-reactor FP behavior possible. Details of the development of HAXPES applicable to the micro particle are described in the next sub-section.

### 2.5.3 HAXPES development for the measurement of samples outside 1F units

We are planning HAXPES study using both synchrotron radiation and laboratory X-ray source. While a synchrotron radiation experiment is advantageous on the points of high S/N and short measuring time due to high photon flux, a laboratory X-ray source experiment is useful on the preliminary test study because it is free from a restriction of beam time. We have been performing HAXPES experiments using synchrotron radiation at JAEA beamline BL22XU of SPring-8 and using laboratory Cr $K_\alpha$ X-ray source (5.4 keV photon energy). The practical energy range of HAXPES experiment at BL22XU is 4 - 10 keV. Moreover, we have been developing new laboratory HAXPES system equipped with Ga $K_\alpha$ X-ray source (9.25 keV photon energy) as a more bulk sensitive system than the Cr $K_\alpha$-HAXPES system. Short exposure times and high throughput are expected for this Ga $K_\alpha$ X-ray source due to higher brightness with an excellent spot quality. In the application of HAXPES on the samples outside 1F units as well as other FP-related samples, charge neutralization of sample surface is vitally important since most of the samples are expected to be insulator and charge-up of sample results in incorrect peak energy position and peak broadening. Through test studies at the BL22XU of SPring-8, we have developed a charge neutralizing method for HAXPES measurement using the combined ion and flood gun, which provide both an electron beam and a low energy ion beam onto the sample surface. This method allowed us to identify the chemical form of Cs-Si-O system from a precise estimate of chemical shifts of Si *1s* core level peak.

## 3. Concluding summary

The results and progress of fundamental research on FP chemistry for the year 2015 were reported. The research has progressed as planned as a whole and has continuously provided fundamental data and knowledge towards the construction of the FP chemistry database. In particular, that of Cs chemisorption was recognized as a useful fundamental knowledge for the 1F decommissioning R&D, which resulted in various invited participation in lectures and speeches at workshops and research committees. The Cs chemisorption study has also been approved as a research theme for an IRID project since JFY 2016.

The research shall continue towards the goal of contributing to both the 1F decommissioning R&D and the enhancement of LWR safety. In addition to the concrete promotion of research, the following points should be taken into consideration for more effective promotion of the research.

- The construction of a Japanese FP research platform is considered essential2), especially for fundamental research. The platform is expected to attract and interact with oversea researchers, providing knowledge on FP behavior. It will also be effective for the promotion of the FP-related research in Japan since such fundamental research basis of FP is currently insufficient in Japan.
- A methodology for elucidating in-reactor FP behavior from the analysis results of samples outside 1F units is interesting approach and a related study is starting from a trial step. Such methodology construction could also contribute to the planning of 1F debris sample analyses.
- Results should continuously be reflected to the research on LWR safety enhancement. For instance, evaluation of FP behavior at the boundary region between in-reactor and outside-reactor, i.e. PCV, S/C, filtered venting system, could be useful. Other issues having large uncertainty should be considered, such as FP release behavior at a re-flooding to the degraded core, sea-water effect on the FP chemistry, behavior of semi-volatile FPs that would be important for 1F issue. As for the latter, for example, Sr release and transport, re-distribution of Mo and Ba in solidified melt under slow cooling condition, etc. would be of interest.

## Acknowledgement

The authors would like to express their appreciation to Messrs. Takada, Ebata and Yonekawa for help in experiment. They also want to thank Dr. Nagase for his continuous support to the FP chemistry research.

References

1) S. Miwa, M. Amaya, K. Tanaka, M. Osaka, F. Nagase : "Research program for the evaluation of fission product and actinide release behavior, focusing on their chemical forms; Position and plan of the research program", JAEA-Review 2013-034 (2013), 42p.

2) Research Team for Fission Product Behavior : "Significance of international cooperative research on fission product behavior towards decommissioning of Fukushima Daiichi Nuclear Power Station; Review of the CLADS International Workshop", JAEA-Review 2016-012 (2016), 17p.

3) Fukushima Project Team, Oarai Research and Development Center, et al. : "Evaluation of fission product and actinide release behavior during BWR severe accident focusing on the chemical forms; 2013 annual report", JAEA-Technology 2014-014 (2014), 60p.

4) F. G. Di Lemma, S. Miwa, M. Osaka : "Boron Release Kinetics from Mixed Melts of Boron Carbide, Stainless Steel and Zircaloy - A Literature Review on the Behavior of Control Rod Materials under Severe Accidents-", JAEA-Review 2016-007 (2016), 27p.

5) K. Minato : "Thermodynamic analysis of cesium and iodine behavior in severe light water reactor accidents", J. Nucl. Mater., 185, pp.154-158 (1991).

6) T. Haste, F. Payot, P. D. W. Bottomley : "Transport and deposition in the Phébus FP circuit", Annals Nucl. Energy, 61, pp.102-121 (2013).

7) S. Miwa, S. Yamashita, M. Osaka : "Prediction of the effects of boron release kinetics on the vapor species of cesium and iodine fission products", Prog. Nucl. Energy, 95, pp.254-259 (2016).

8) S. Miwa, G. Ducros, E. Hanus, P. D. W. Bottomley, S. Van Winckel : "Upgrading the experimental database of fission products and actinides release behaviour in the VERCORS program through chemical analysis", Proc. 7th European Review Meeting on Severe Accident Research (ERMSAR 2015), March 24-26, 2015, Marseille, France, (2015).

9) M. R. Kuhlman, D. J. Lehmicke, R. O. Meyer : "CORSOR User's Manual", NUREG/CR-4173, (1985).

10) Y. Pontillon, G. Ducros : "Behaviour of fission products under severe PWR accident conditions. The VERCORS experimental programme - Part 2: Release and transport of fission gases and volatile fission products", Nucl. Eng. Design, 240, pp.1853-1866 (2010).

11) T. Kudo, M. Kida, T. Nakamura, F. Nagase, T. Fuketa : "Releases of Cesium and Poorly Volatile Elements from $UO_2$ and MOX Fuels under Severe Accident Conditions", J. Nucl. Sci. Technol., 44(11), pp.1421-1427 (2007).

12) F. G. Di Lemma, S. Miwa, J. Takada, M. Takano, M. Osaka : "Evaluation of FP Chemistry under Severe Accident Conditions with Focuses on the Effects of BWR Control

Material (6) Oxidation behavior of $B_4C$/SS/Zry mixed melts phases", Proceedings of AESJ 2016 Fall Meeting, Presentation No. 2B17, (2016).

13) M. Takano, T. Nishi, N. Shirasu : "Characterization of solidified melt among materials of $UO_2$ fuel and $B_4C$ control blade", J. Nucl. Sci. Technol., 51(7-8), pp.859-875 (2014).

14) L. Cantrel, E. Krausmann : "Reaction kinetics of a fission-product mixture in a steam-hydrogen carrier gas in the Phebus primary circuit", Nucl. Technol., 144, pp.1-16 (2003).

15) S. Miwa, M. Osaka, G. Ducros, E. Hanus : "Evaluation of FP Chemistry under Severe Accident Conditions with Focuses on the Effects of BWR Control Material (2) Effect of atmosphere on the FP release and transport behavior", Proceedings of AESJ 2015 Fall Meeting, Presentation No. J09, (2015).

16) S. Miwa, M. Shinada, M. Osaka, T. Sugiyama, Y. Maruyama : "Evaluation of FP chemistry for improvement of source term estimation method (1) Experimental evaluation of B effects on revaporization behavior of Cs and I", Proceedings of AESJ 2016 Fall Meeting, Presentation No. 2G14, (2016).

17) J. Kalilainen, T. Kärkelä, R. Zilliacus, U. Tapper, A. Auvinen, J. Jokiniemi : "Chemical reactions of fission product deposits and iodine transport in primary circuit conditions", Nucl. Eng. Design, 267, pp.140-147 (2014).

18) T. Wangle, V. Tyrpekl, M. Cologna, J. Somers : "Simulated $UO_2$ fuel containing CsI by Spark Plasma Sintering", J. Nucl. Mater., 466, pp.150-153 (2015).

19) Y. Takamatsu, K. Kurosaki, H. Ishii, M. Osaka, K. Nakajima, S. Miwa, F. G. Di Lemma, Y. Ohishi, H. Muta, S. Yamanaka : "Synthesis of $CeO_2$ based simulated fuel containing CsI to evaluate the release behavior of Cs and I", Proceedings of AESJ 2016 Fall Meeting, Presentation No. 3B11, (2016).

20) F. G. Di Lemma, K. Nakajima, S. Yamashita, M. Osaka : "Surface analyses of cesium hydroxide chemisorbed onto type 304 stainless steel", Nucl. Eng. Design, 305, pp.411-420 (2016).

21) F. G. Di Lemma, K. Nakajima, S. Yamashita, M. Osaka, F. Nagase : "Experimental studies on CsOH chemisorption onto stainless steel samples, as simulate reactor structural materials", Submission ID 124, IYNC2016, Hangzhou, China, July 24-30, (2016).

22) G. Kresse, J. Hafner : "Ab initio molecular dynamics for liquid metals", Phys. Rev. B, 47, pp.558-561 (1993).

23) N. Girault, F. Payot : "Insights into iodine behaviour and speciation in the Phebus primary circuit", Annals Nucl. Energy, 61, pp.143-156 (2013).

24) A. B. Kaplun, A. B. Meshalkin : “Phase equilibria in the binary systems $Li_2O$‐$B_2O_3$ and $Cs_2O$‐$B_2O_3$”, J. Cryst. Growth, 209, pp.890-894 (2000).

25) N. Penin, M. Touboul, G. Nowogrocki : “New form of the $Cs_2O$‐$B_2O_3$ phase diagram”, J. Cryst. Growth, 256(3-4), pp.334-340 (2003).

26) G. Nowogrocki, N. Penin, M. Touboul : “Crystal structure of $Cs_3B_7O_{12}$ containing a new large polyanion with 63 boron atoms”, Solid State Sci., 5(5), pp.795-803 (2003).

27) R. S. Bubnova, S. V. Krivovichev, I. P. Shakhverdova, S. K. Filatov, P. C. Burns, M. G. Krzhizhanovskaya, I. G. Polyakova : “Synthesis, crystal structure and thermal behavior of $Rb_3B_7O_{12}$, a new compound”, Solid State Sci., 4(7), pp.985-992 (2002).

28) R. G. J. Ball, B. R. Bowsher, E. H. P. Cordfunke, S. Dickinson, R. J. M. Konings : “Thermochemistry of selected fission product compounds”, J. Nucl. Mater., 201(2), pp.81-91 (1993).

29) P. F. Henry, M. T. Weller : “$CsFeSiO_4$: a maximum iron content zeotype”, Chem. Commun., 24, pp.2723-2724 (1998).

30) B. Clement : “Towards reducing the uncertainties on Source Term Evaluations: an IRSN/CEA/EDF R&D programme”, Proceedings of EUROSAFE2004, Berlin, Germany, November 8-9, (2004).

31) ANSYS® Fluent®, Release 17.2.

32) CHEMKIN 15151, ANSYS Reaction Design: San Diego, (2016).

33) Y. Iwata, C. Ito, S. Yamashita, M. Osaka : “Evaluation of FP Chemistry under Severe Accident Conditions with Focuses on the Effects of BWR Control Material - (5) Development of analysis technique of boron and iodine in cesium species using laser resonance ionization”, Proceedings of AESJ 2015 Fall Meeting, Presentation No. J12, (2015).

34) T. Okane, M. Kobata, I. Sato, K. Kobayashi, M. Osaka, H. Yamagami : “Hard X-ray photoelectron spectroscopy study for transport behavior of CsI in heating test simulating a BWR severe accident condition: Chemical effects of boron vapors”, Nucl. Eng. Design, 297, pp.251-256 (2016).

35) M. Iwasaki, K. Tanaka, I. Sato, S. Miwa, M. Osaka, M. Amaya, S. Koyama, T. Seki, D. Tokoro, T. Ishigamori : “Evaluation of fission product release and transport behavior during severe accident focusing on the chemical forms, 4; Development of "in situ" measurement technology for evaluating chemical form of released FP”, Proceedings of AESJ 2014 Fall Meeting, Presentation No. C04, (2014).

36) K. Adachi, M. Kajino, Y. Zaizen, Y. Igarashi : “Emission of spherical cesium-bearing

particles from an early stage of the Fukushima nuclear accident", Sci. Reports, 3, Article number: 2554 (2013).

37) Y. Abe, Y. Iizawa, Y. Terada, K. Adachi, Y. Igarashi, I. Nakai : "Detection of Uranium and Chemical State Analysis of Individual Radioactive Microparticles Emitted from the Fukushima Nuclear Accident Using Multiple Synchrotron Radiation X-ray Analyses", Analytical Chem., 86(17), pp.8521-8525 (2014).

38) Y. Satou, K. Sueki, K. Sasa, K. Adachi, Y. Igarashi : "First successful isolation of radioactive particles from soil near the Fukushima Daiichi Nuclear Power Plant", Anthropocene, 14, pp.71-76 (2016).

39) N. Yamaguchi, M. Mitome, Akiyama-Hasegawa Kotone, M. Asano, K. Adachi, T. Kogure : "Internal structure of cesium-bearing radioactive microparticles released from Fukushima nuclear power plant", Sci. Reports, 6, Article number: 20548 (2016).

40) M. Asami, H. Watahiki, T. Ohi, A. Shibata, T. Ashida : "Analysis Results of Contaminated Water and Rubbles/Soils in Fukushima Daiichi Nuclear Power Station - The Release of FY2014 Edition of the Analysis Results of Contaminated Water and Rubbles/Soils -", JAEA-Data/Code 2015-020, (2015), 80p.

41) K. Maeda, S. Sasaki, M. Kumai, I. Sato, M. Suto, M. Ohsaka, T. Goto, H. Sakai, T. Chigira, H. Murata : "Distribution of radioactive nuclides of boring core samples extracted from concrete structures of reactor buildings in the Fukushima Daiichi Nuclear Power Plant", J. Nucl. Sci. Technol., 51, pp.1006-1023 (2014).

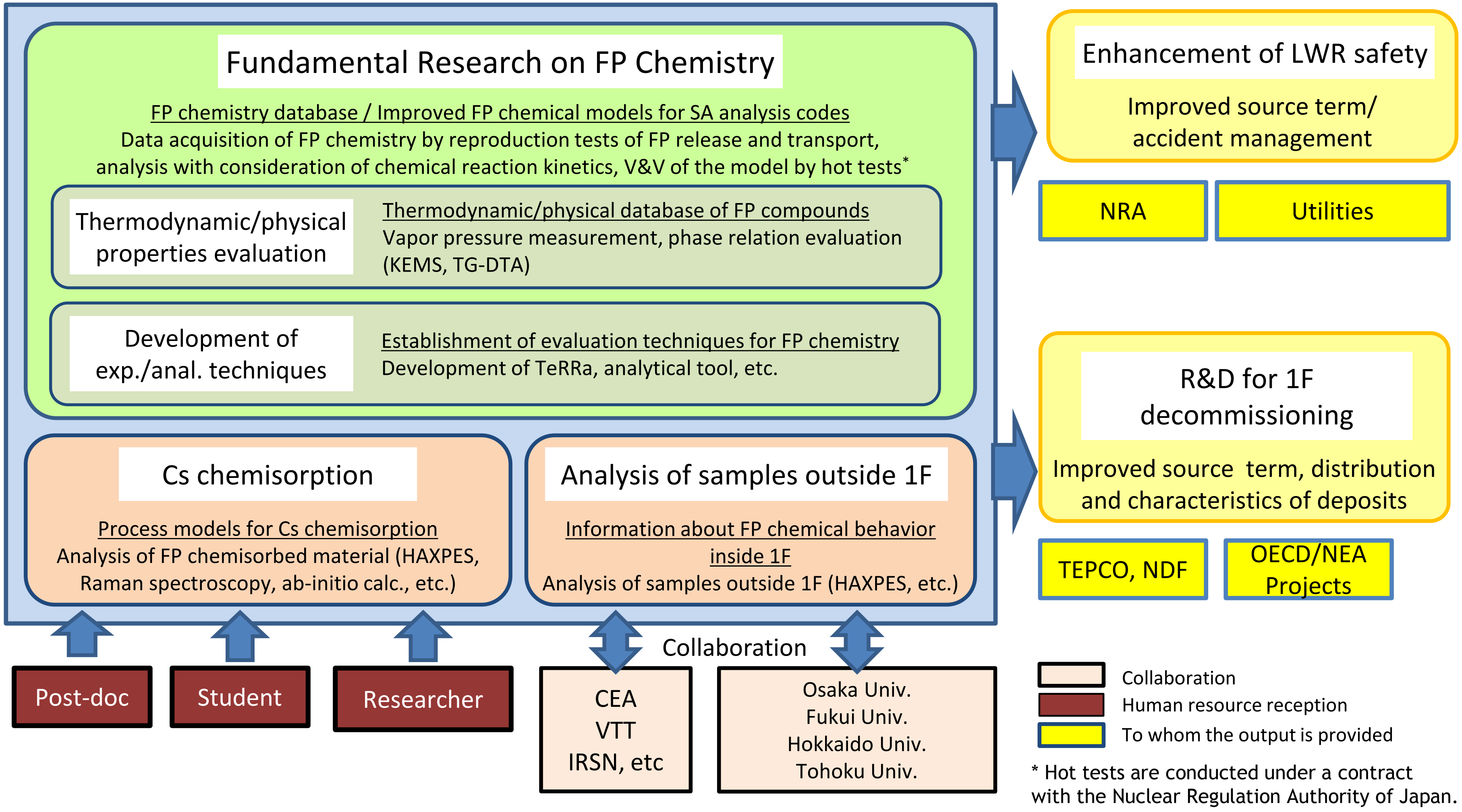

Fig. 1 Organization for the fundamental research on FP chemistry

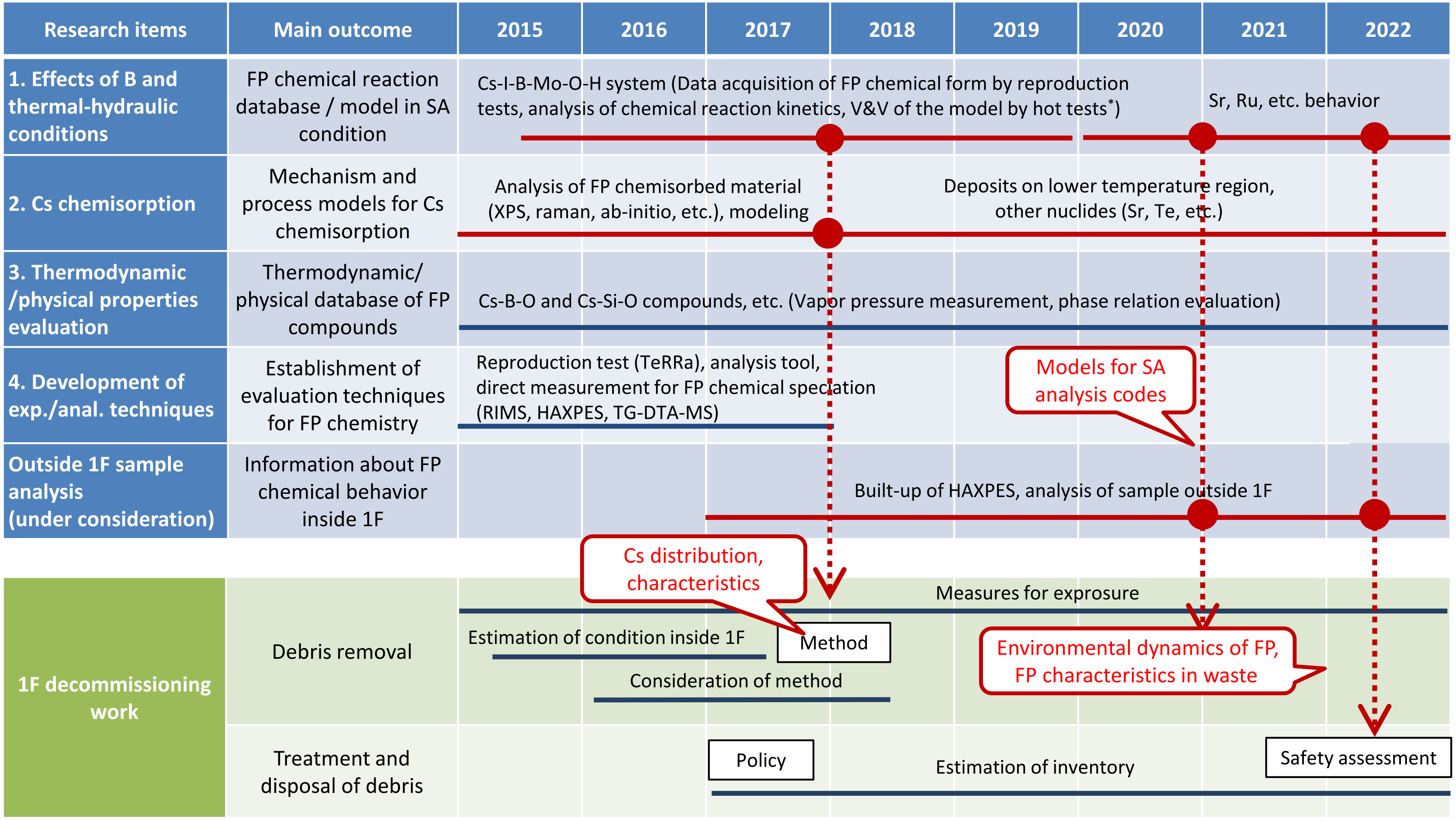

* Hot tests are conducted under a contract with the Nuclear Regulation Authority of Japan.

**Fig. 2 Mid-term plan for the fundamental research on FP chemistry**

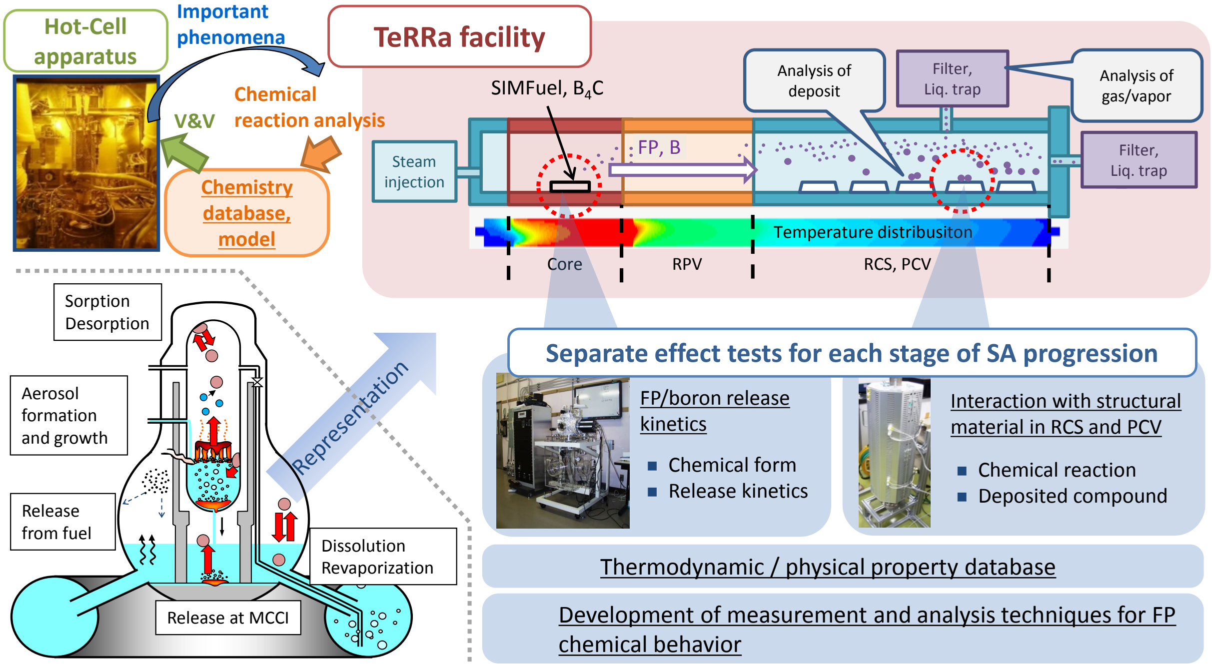

Fig. 3 Main framework of the fundamental research on FP chemistry

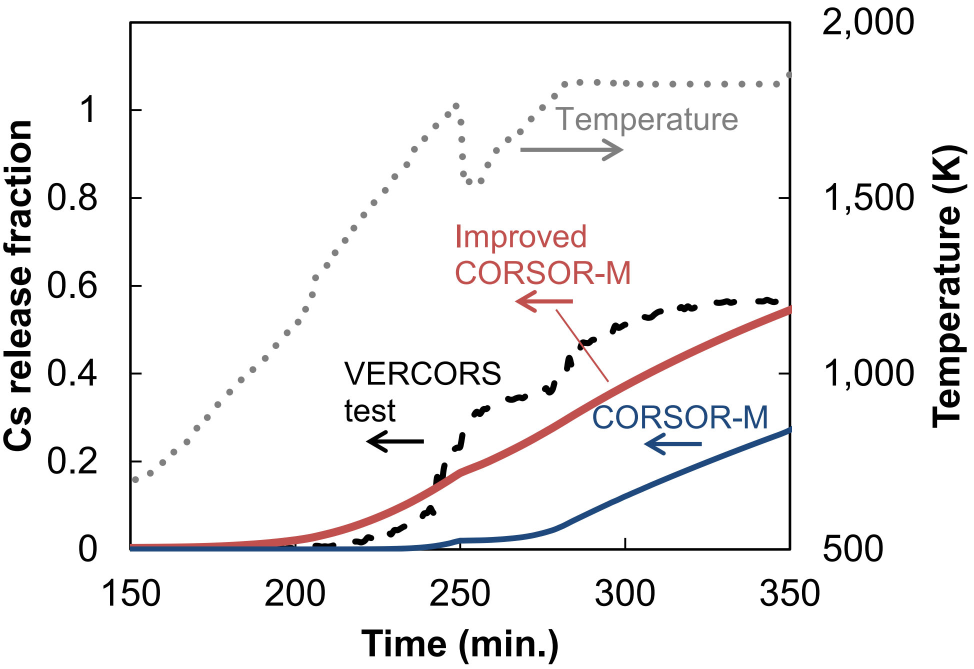

Fig. 4 Reproduction of Cs release rate from MOX fuel in the VERCOR test by the improved CORSOR-M model for MOX fuel

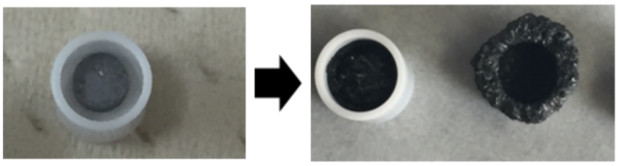

As prepared

After the test in Ar-$H_2O$
at 1,173 K (left) and 1,373 K (right)

Fig. 5 Appearance of prepared FeB sample used in the oxidation and vaporization tests in the B-ReK facility

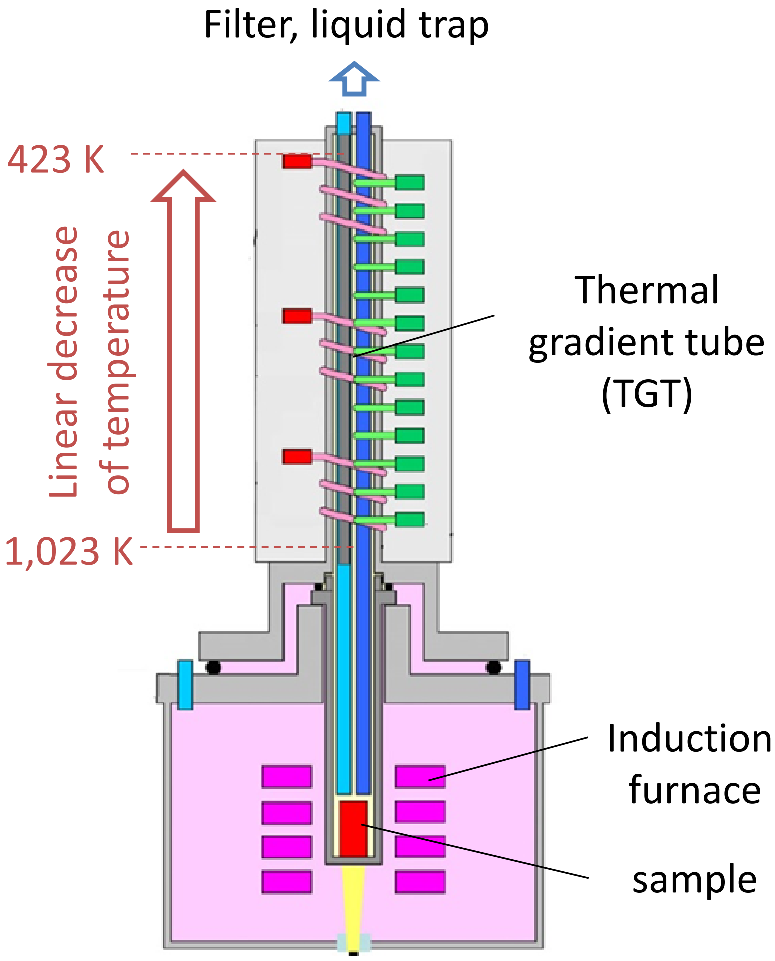

Fig. 6 Schematic view of a small size test facility for FP release and transport

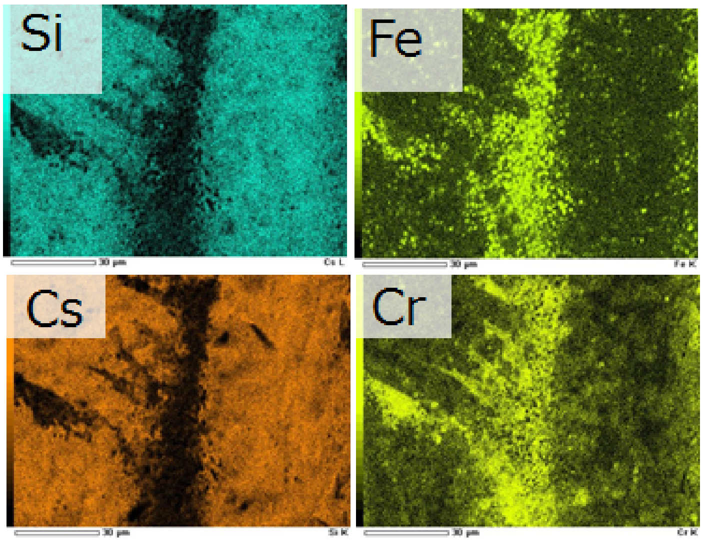

Fig. 7 An example of elemental distribution on the surface of SS304 exposed to CsOH vapor[21)]

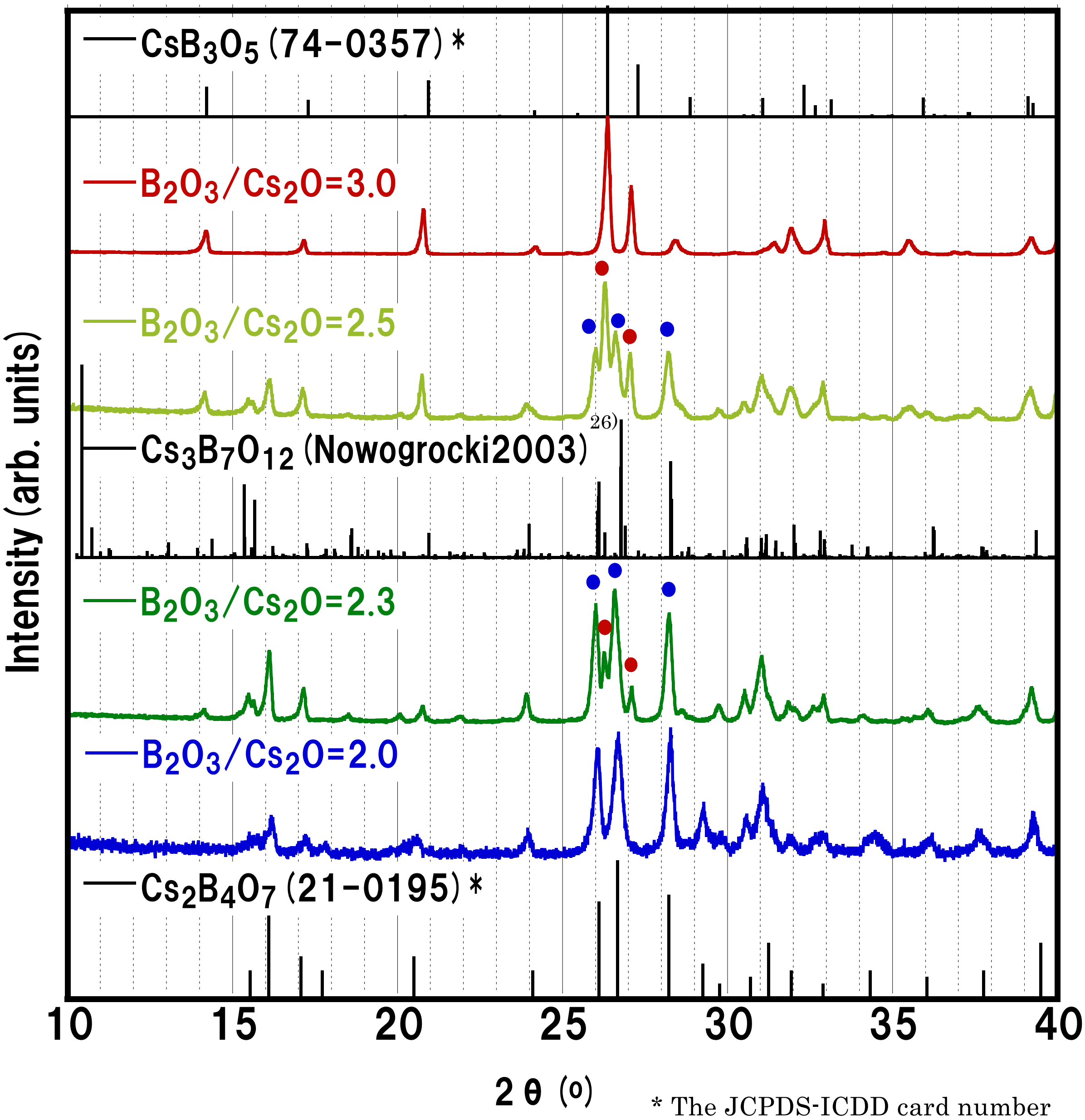

* The JCPDS-ICDD card number

Fig. 8 X-Ray diffraction patterns of synthesized $Cs_2B_4O_7$ and $CsB_3O_5$ at room temperature

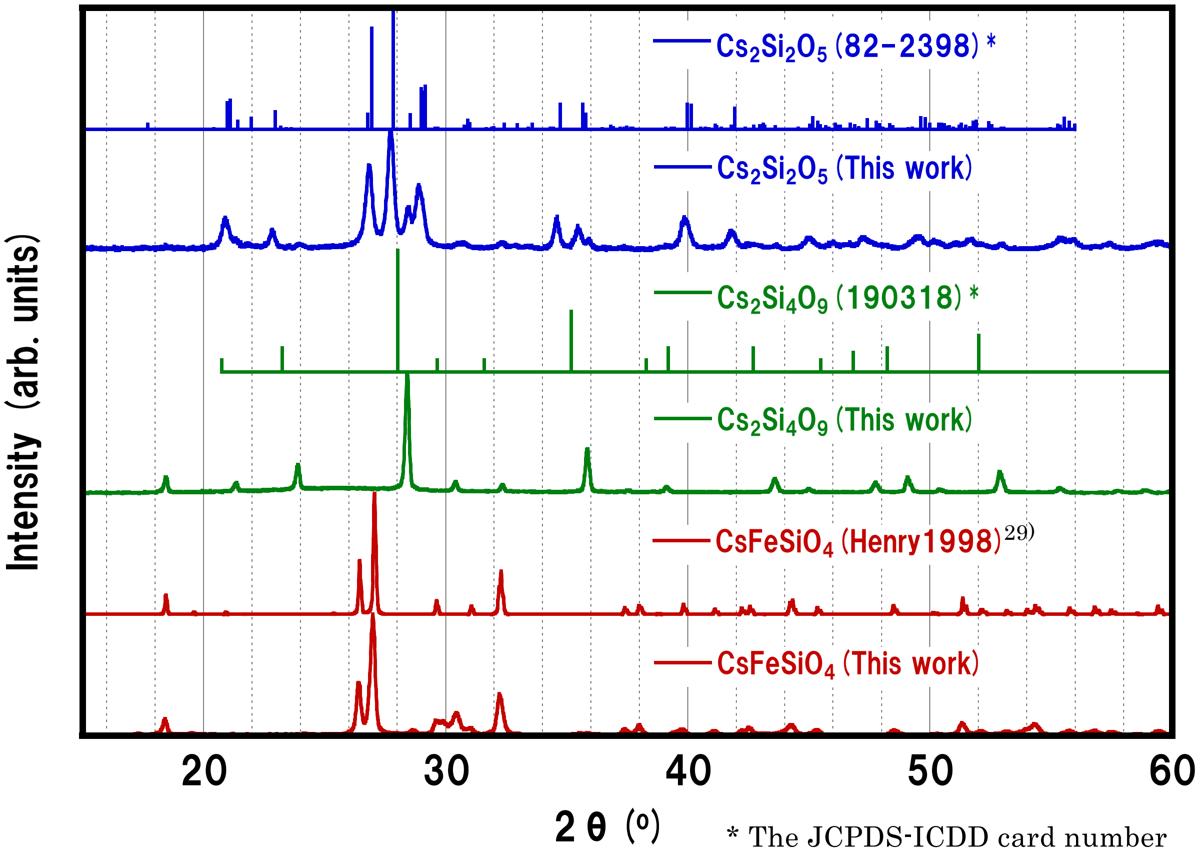

* The JCPDS-ICDD card number

Fig. 9 X-ray diffraction patterns of synthesized $Cs_2Si_2O_5$, $Cs_2Si_4O_9$ and $CsFeSiO_4$

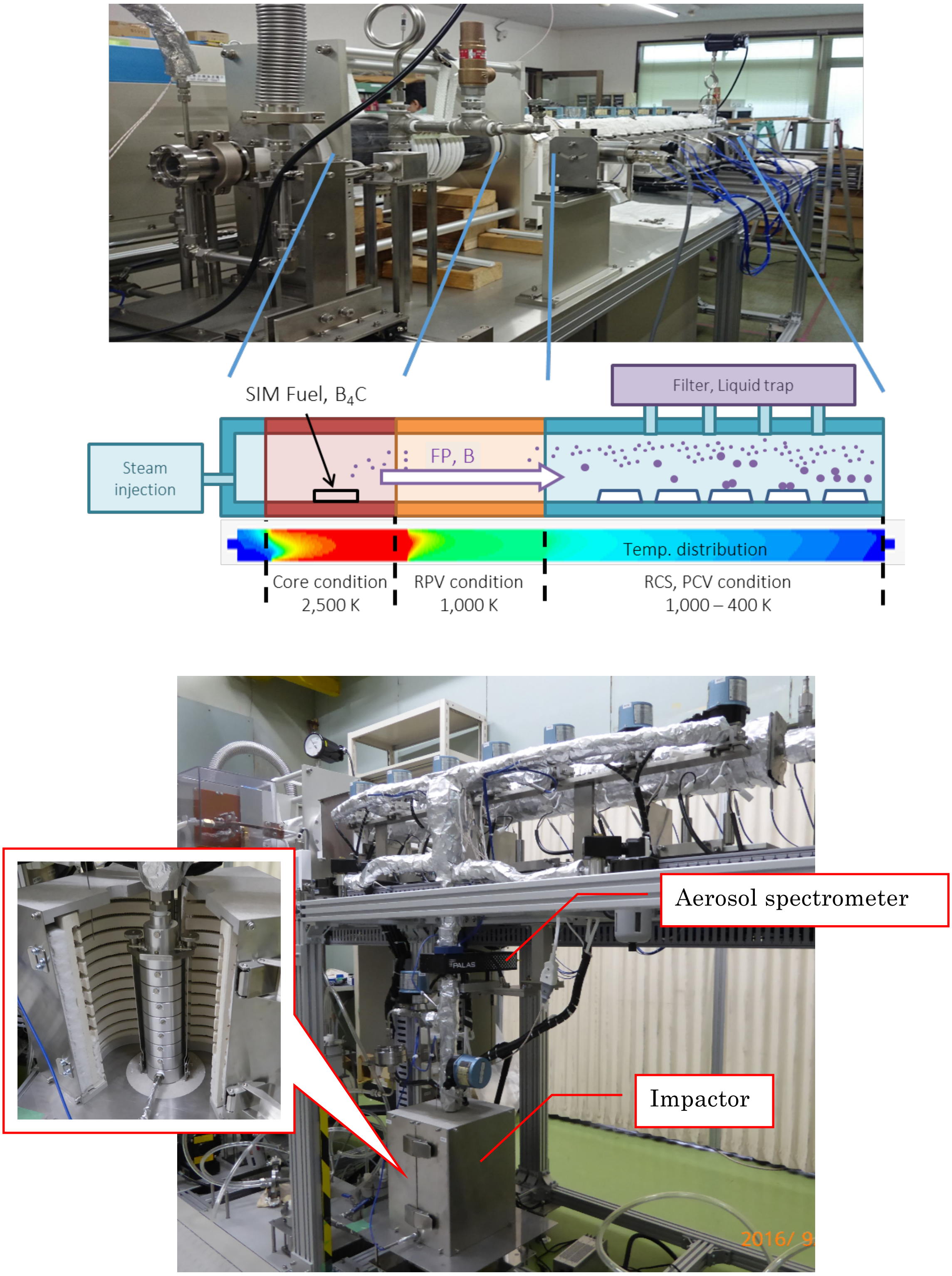

Fig. 10 Appearance of and FP flow in TeRRa facility

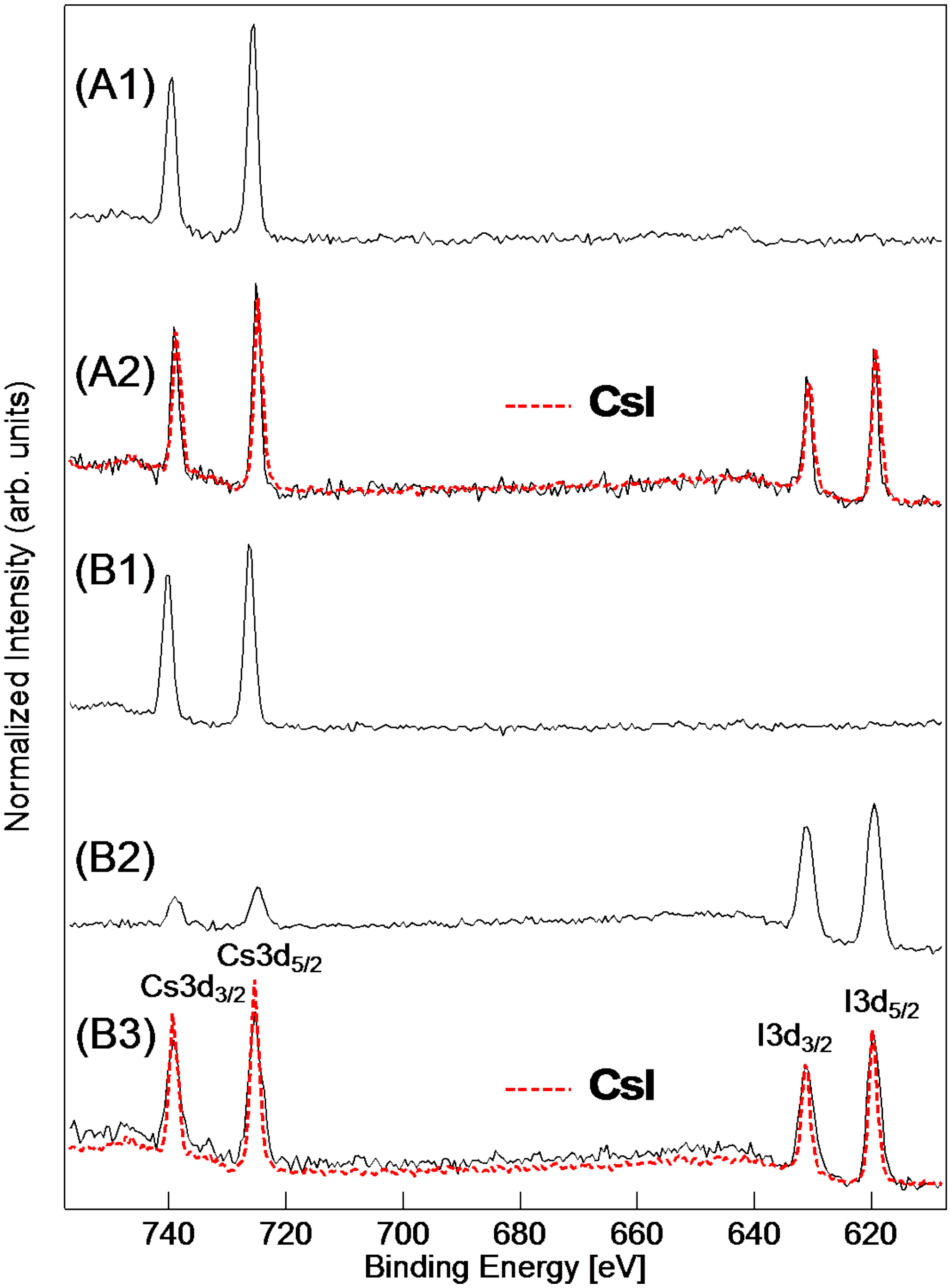

Fig. 11 HAXPES spectra of Cs 3*d* and I 3*d* core levels for the thermal gradient tube (TGT) samples of (A1) TGT at ~ 650°C, not exposed to $B_2O_3$ vapor, (A2) TGT at ~ 300°C, not exposed to $B_2O_3$ vapor, (B1) TGT at ~ 650°C, exposed to $B_2O_3$ vapor, (B2) TGT at ~ 300°C, exposed to $B_2O_3$ vapor, and (B3) TGT at ~ 150°C, exposed to $B_2O_3$ vapor. Red broken lines are HAXPES spectrum for CsI reference.

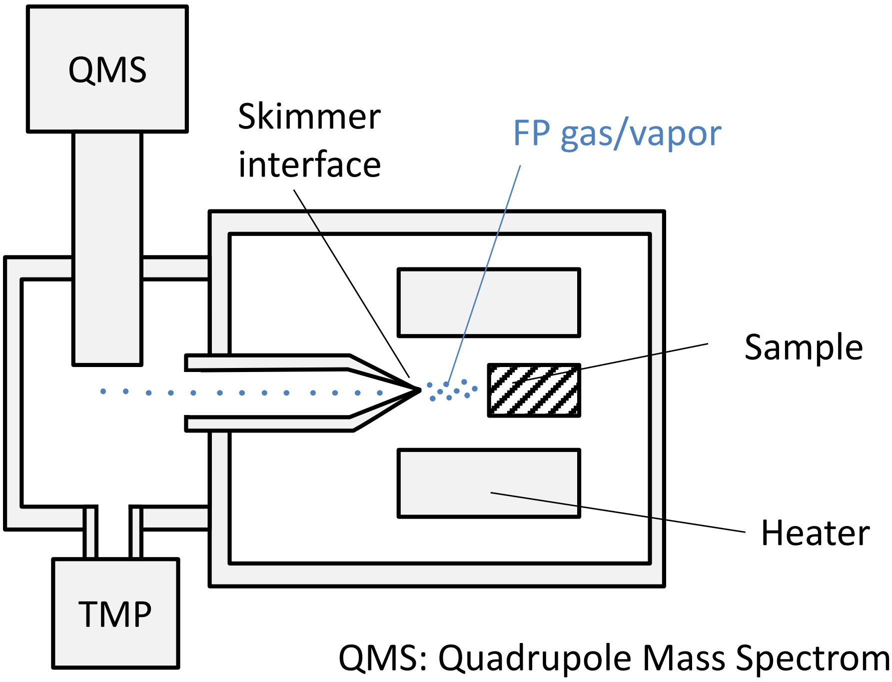

QMS: Quadrupole Mass Spectrometer
TMP: Turbo Molecular Pump

Fig. 12 Schematic diagram of TG-DTA-MS apparatus

Table 1 Breakdown structure of research

| Research items | Main output | Contents of the evaluation | 4. Development of experimental and analytical techniques for the FP chemistry research |
|---|---|---|---|
| 1. Evaluation of effects of B release kinetics and thermal-hydraulic conditions on FP chemistry | | | |
| FP chemical behavior from RPV to PCV | Fundamental data/knowledge on FP chemical behaviors | Effects of B release kinetics, atmosphere and MOX fuel on FP chemical behaviors | - Reproduction test techniques for FP release and transport<br>- Analytical tool incorporating chemical reaction kinetics treatment<br>- Resonance Ionization Mass Spectrometry (RIMS) for direct measurement of chemical form<br>- Hard X-ray Photoelectron Spectroscopy (HAXPES) as a direct evaluation technique of FP chemical states in deposits<br>- TG-DTA-MS apparatus for the direct determination of FP vapor species |
| Boron release kinetics from the $B_4C$-SS-Zry mixed melt | B release model from $B_4C$-SUS-Zry melt | Oxidation and vaporization kinetics of $B_4C$-SUS-Zry melt | |
| Consideration on the effects of chemical reaction kinetics | Basic database on FP chemical reaction kinetics | FP chemical reaction kinetics using reproduction test facility and analytical tool | |
| Synthesis of Cs-containing artificial fuel | Preparation of sufficient samples for systematic FP release and transport tests | Synthesis conditions and characteristics of the artificial fuel | |
| Evaluation of FP behavior at PCV region | Improved boundary conditions for FP release into environment | Aerosol properties, morphology, chemical composition, solubility | |
| 2. Fundamental study on the Cs chemisorption behavior | | | |
| Basic characteristics of Cs chemisorbed compounds | Cs chemisorption model | Effect of the atmosphere and other FPs and released materials during a SA (e.g. Mo, and B) on the chemisorption mechanism | - HAXPES as a direct evaluation technique of FP chemical states in deposits<br>- Experimental technique under high pressure conditions |
| Ab-initio study on the chemisorbed Cs-Si-Fe-O compounds | An evidence for Cs chemisorbed compounds | Stability of Cs chemisorbed compounds | |
| 3. Enlargement of a database on thermodynamic and thermophysical properties of FP compounds | | | |
| Cs-Si-O / Cs-B-O system | Thermodynamic and thermophysical database | Thermodynamic data and phase relation | |

Table 2 Changes in formation of B, Cs and I species under a steam-starvation atmosphere due to the decrease in B release from the mixed melt of $B_4C$-SS-Zry[7)]

| Relative change in amounts | |
|---|---|
| $CsBO_2$ | - 97% |
| CsI | + 17% |
| HI | - 30% |
| I | - 30% |

Table 3 Calculation results of the changes of Cs chemical species through the RCS to PCV

| | Release temperature from fuel | Cs and I chemical species just after release | Cs and I chemical species in deposits | | |
|---|---|---|---|---|---|
| | | | > 800 K | 800 – 600 K | < 600 K |
| Steam atmosphere (VERCORS -HT2) | < 2,200 K | CsOH,<br>$CsBO_2$,<br>$Cs_2MoO_4$ | $CsBO_2$,<br>$Cs_2MoO_4$ | CsOH | CsOH |
| | > 2,200 K | $CsBO_2$,<br>CsOH | $CsBO_2$ | CsOH | Cs |
| Hydrogen atmosphere (VERCORS -HT3) | < 2,200 K | Cs,<br>$CsBO_2$,<br>CsI | $CsBO_2$,<br>$Cs_2Te$ | CsI | Cs |
| | > 2,200 K | Cs | Little deposits | CsI | Cs |

Table 4 Stability evaluation on Cs-Si-Fe-O compounds by ab-initio calculation

| Compound | System | Energy |
|---|---|---|
| Reference | $Cs_2O + 4SiO_2 + Fe_2O_3$ | - |
| $Cs_2Si_2O_5$ | $Cs_2Si_2O_5 + 2SiO_2 + Fe_2O_3$ | Highest |
| $Cs_2Si_4O_9$ | $Cs_2Si_4O_9 + Fe_2O_3$ | Second highest |
| $CsSiFeO_4$ | $2CsSiFeO_4 + 2SiO_2$ | Second lowest |
| $CsSi_2FeO_6$ | $2CsSi_2FeO_6$ | Lowest |

# 国際単位系（SI）

表１．SI 基本単位

| 基本量 | SI 基本単位 | |
|---|---|---|
| | 名称 | 記号 |
| 長さ | メートル | m |
| 質量 | キログラム | kg |
| 時間 | 秒 | s |
| 電流 | アンペア | A |
| 熱力学温度 | ケルビン | K |
| 物質量 | モル | mol |
| 光度 | カンデラ | cd |

表２．基本単位を用いて表されるSI組立単位の例

| 組立量 | SI 組立単位 | |
|---|---|---|
| | 名称 | 記号 |
| 面積 | 平方メートル | m$^2$ |
| 体積 | 立方メートル | m$^3$ |
| 速さ，速度 | メートル毎秒 | m/s |
| 加速度 | メートル毎秒毎秒 | m/s$^2$ |
| 波数 | 毎メートル | m$^{-1}$ |
| 密度，質量密度 | キログラム毎立方メートル | kg/m$^3$ |
| 面積密度 | キログラム毎平方メートル | kg/m$^2$ |
| 比体積 | 立方メートル毎キログラム | m$^3$/kg |
| 電流密度 | アンペア毎平方メートル | A/m$^2$ |
| 磁界の強さ | アンペア毎メートル | A/m |
| 量濃度(a)，濃度 | モル毎立方メートル | mol/m$^3$ |
| 質量濃度 | キログラム毎立方メートル | kg/m$^3$ |
| 輝度 | カンデラ毎平方メートル | cd/m$^2$ |
| 屈折率(b) | （数字の） 1 | 1 |
| 比透磁率(b) | （数字の） 1 | 1 |

(a) 量濃度（amount concentration）は臨床化学の分野では物質濃度（substance concentration）ともよばれる。

(b) これらは無次元量あるいは次元１をもつ量であるが、そのことを表す単位記号である数字の１は通常は表記しない。

表３．固有の名称と記号で表されるSI組立単位

| 組立量 | SI 組立単位 | | | |
|---|---|---|---|---|
| | 名称 | 記号 | 他のSI単位による表し方 | SI基本単位による表し方 |
| 平面角 | ラジアン(b) | rad | 1 (b) | m/m |
| 立体角 | ステラジアン(b) | sr(c) | 1 (b) | m$^2$/m$^2$ |
| 周波数 | ヘルツ(d) | Hz | | s$^{-1}$ |
| 力 | ニュートン | N | | m kg s$^{-2}$ |
| 圧力，応力 | パスカル | Pa | N/m$^2$ | m$^{-1}$ kg s$^{-2}$ |
| エネルギー，仕事，熱量 | ジュール | J | N m | m$^2$ kg s$^{-2}$ |
| 仕事率，工率，放射束 | ワット | W | J/s | m$^2$ kg s$^{-3}$ |
| 電荷，電気量 | クーロン | C | | s A |
| 電位差（電圧），起電力 | ボルト | V | W/A | m$^2$ kg s$^{-3}$ A$^{-1}$ |
| 静電容量 | ファラド | F | C/V | m$^{-2}$ kg$^{-1}$ s$^4$ A$^2$ |
| 電気抵抗 | オーム | Ω | V/A | m$^2$ kg s$^{-3}$ A$^{-2}$ |
| コンダクタンス | ジーメンス | S | A/V | m$^{-2}$ kg$^{-1}$ s$^3$ A$^2$ |
| 磁束 | ウエーバ | Wb | Vs | m$^2$ kg s$^{-2}$ A$^{-1}$ |
| 磁束密度 | テスラ | T | Wb/m$^2$ | kg s$^{-2}$ A$^{-1}$ |
| インダクタンス | ヘンリー | H | Wb/A | m$^2$ kg s$^{-2}$ A$^{-2}$ |
| セルシウス温度 | セルシウス度(e) | ℃ | | K |
| 光束 | ルーメン | lm | cd sr(c) | cd |
| 照度 | ルクス | lx | lm/m$^2$ | m$^{-2}$ cd |
| 放射性核種の放射能(f) | ベクレル(d) | Bq | | s$^{-1}$ |
| 吸収線量, 比エネルギー分与, カーマ | グレイ | Gy | J/kg | m$^2$ s$^{-2}$ |
| 線量当量, 周辺線量当量, 方向性線量当量, 個人線量当量 | シーベルト(g) | Sv | J/kg | m$^2$ s$^{-2}$ |
| 酸素活性 | カタール | kat | | s$^{-1}$ mol |

(a)SI接頭語は固有の名称と記号を持つ組立単位と組み合わせても使用できる。しかし接頭語を付した単位はもはやコヒーレントではない。

(b)ラジアンとステラジアンは数字の１に対する単位の特別な名称で、量についての情報をつたえるために使われる。実際には、使用する時には記号rad及びsrが用いられるが、習慣として組立単位としての記号である数字の１は明示されない。

(c)測光学ではステラジアンという名称と記号srを単位の表し方の中に、そのまま維持している。

(d)ヘルツは周期現象についてのみ、ベクレルは放射性核種の統計的過程についてのみ使用される。

(e)セルシウス度はケルビンの特別な名称で、セルシウス温度を表すために使用される。セルシウス度とケルビンの単位の大きさは同一である。したがって、温度差や温度間隔を表す数値はどちらの単位で表しても同じである。

(f)放射性核種の放射能（activity referred to a radionuclide）は、しばしば誤った用語で”radioactivity”と記される。

(g)単位シーベルト（PV,2002,70,205）についてはCIPM勧告2（CI-2002）を参照。

表４．単位の中に固有の名称と記号を含むSI組立単位の例

| 組立量 | SI 組立単位 | | |
|---|---|---|---|
| | 名称 | 記号 | SI 基本単位による表し方 |
| 粘度 | パスカル秒 | Pa s | m$^{-1}$ kg s$^{-1}$ |
| 力のモーメント | ニュートンメートル | N m | m$^2$ kg s$^{-2}$ |
| 表面張力 | ニュートン毎メートル | N/m | kg s$^{-2}$ |
| 角速度 | ラジアン毎秒 | rad/s | m m$^{-1}$ s$^{-1}$=s$^{-1}$ |
| 角加速度 | ラジアン毎秒毎秒 | rad/s$^2$ | m m$^{-1}$ s$^{-2}$=s$^{-2}$ |
| 熱流密度，放射照度 | ワット毎平方メートル | W/m$^2$ | kg s$^{-3}$ |
| 熱容量，エントロピー | ジュール毎ケルビン | J/K | m$^2$ kg s$^{-2}$ K$^{-1}$ |
| 比熱容量，比エントロピー | ジュール毎キログラム毎ケルビン | J/(kg K) | m$^2$ s$^{-2}$ K$^{-1}$ |
| 比エネルギー | ジュール毎キログラム | J/kg | m$^2$ s$^{-2}$ |
| 熱伝導率 | ワット毎メートル毎ケルビン | W/(m K) | m kg s$^{-3}$ K$^{-1}$ |
| 体積エネルギー | ジュール毎立方メートル | J/m$^3$ | m$^{-1}$ kg s$^{-2}$ |
| 電界の強さ | ボルト毎メートル | V/m | m kg s$^{-3}$ A$^{-1}$ |
| 電荷密度 | クーロン毎立方メートル | C/m$^3$ | m$^{-3}$ s A |
| 表面電荷 | クーロン毎平方メートル | C/m$^2$ | m$^{-2}$ s A |
| 電束密度，電気変位 | クーロン毎平方メートル | C/m$^2$ | m$^{-2}$ s A |
| 誘電率 | ファラド毎メートル | F/m | m$^{-3}$ kg$^{-1}$ s$^4$ A$^2$ |
| 透磁率 | ヘンリー毎メートル | H/m | m kg s$^{-2}$ A$^{-2}$ |
| モルエネルギー | ジュール毎モル | J/mol | m$^2$ kg s$^{-2}$ mol$^{-1}$ |
| モルエントロピー, モル熱容量 | ジュール毎モル毎ケルビン | J/(mol K) | m$^2$ kg s$^{-2}$ K$^{-1}$ mol$^{-1}$ |
| 照射線量（X線及びγ線） | クーロン毎キログラム | C/kg | kg$^{-1}$ s A |
| 吸収線量率 | グレイ毎秒 | Gy/s | m$^2$ s$^{-3}$ |
| 放射強度 | ワット毎ステラジアン | W/sr | m$^4$ m$^{-2}$ kg s$^{-3}$=m$^2$ kg s$^{-3}$ |
| 放射輝度 | ワット毎平方メートル毎ステラジアン | W/(m$^2$ sr) | m$^2$ m$^{-2}$ kg s$^{-3}$=kg s$^{-3}$ |
| 酵素活性濃度 | カタール毎立方メートル | kat/m$^3$ | m$^{-3}$ s$^{-1}$ mol |

表５．SI 接頭語

| 乗数 | 名称 | 記号 | 乗数 | 名称 | 記号 |
|---|---|---|---|---|---|
| $10^{24}$ | ヨタ | Y | $10^{-1}$ | デシ | d |
| $10^{21}$ | ゼタ | Z | $10^{-2}$ | センチ | c |
| $10^{18}$ | エクサ | E | $10^{-3}$ | ミリ | m |
| $10^{15}$ | ペタ | P | $10^{-6}$ | マイクロ | µ |
| $10^{12}$ | テラ | T | $10^{-9}$ | ナノ | n |
| $10^{9}$ | ギガ | G | $10^{-12}$ | ピコ | p |
| $10^{6}$ | メガ | M | $10^{-15}$ | フェムト | f |
| $10^{3}$ | キロ | k | $10^{-18}$ | アト | a |
| $10^{2}$ | ヘクト | h | $10^{-21}$ | ゼプト | z |
| $10^{1}$ | デカ | da | $10^{-24}$ | ヨクト | y |

表６．SIに属さないが、SIと併用される単位

| 名称 | 記号 | SI 単位による値 |
|---|---|---|
| 分 | min | 1 min=60 s |
| 時 | h | 1 h =60 min=3600 s |
| 日 | d | 1 d=24 h=86 400 s |
| 度 | ° | 1°=(π/180) rad |
| 分 | ’ | 1’=(1/60)°=(π/10 800) rad |
| 秒 | ” | 1”=(1/60)’=(π/648 000) rad |
| ヘクタール | ha | 1 ha=1 hm$^2$=10$^4$m$^2$ |
| リットル | L，l | 1 L=1 l=1 dm$^3$=10$^3$cm$^3$=10$^{-3}$m$^3$ |
| トン | t | 1 t=10$^3$ kg |

表７．SIに属さないが、SIと併用される単位で、SI単位で表される数値が実験的に得られるもの

| 名称 | 記号 | SI 単位で表される数値 |
|---|---|---|
| 電子ボルト | eV | 1 eV=1.602 176 53(14)×10$^{-19}$J |
| ダルトン | Da | 1 Da=1.660 538 86(28)×10$^{-27}$kg |
| 統一原子質量単位 | u | 1 u=1 Da |
| 天文単位 | ua | 1 ua=1.495 978 706 91(6)×10$^{11}$m |

表８．SIに属さないが、SIと併用されるその他の単位

| 名称 | 記号 | SI 単位で表される数値 |
|---|---|---|
| バール | bar | 1 bar=0.1MPa=100 kPa=10$^5$Pa |
| 水銀柱ミリメートル | mmHg | 1 mmHg≈133.322Pa |
| オングストローム | Å | 1 Å=0.1nm=100pm=10$^{-10}$m |
| 海里 | M | 1 M=1852m |
| バーン | b | 1 b=100fm$^2$=(10$^{-12}$cm)$^2$=10$^{-28}$m$^2$ |
| ノット | kn | 1 kn=(1852/3600)m/s |
| ネーパ | Np | SI単位との数値的な関係は、対数量の定義に依存。 |
| ベル | B | |
| デシベル | dB | |

表９．固有の名称をもつCGS組立単位

| 名称 | 記号 | SI 単位で表される数値 |
|---|---|---|
| エルグ | erg | 1 erg=10$^{-7}$ J |
| ダイン | dyn | 1 dyn=10$^{-5}$N |
| ポアズ | P | 1 P=1 dyn s cm$^{-2}$=0.1Pa s |
| ストークス | St | 1 St =1cm$^2$ s$^{-1}$=10$^{-4}$m$^2$ s$^{-1}$ |
| スチルブ | sb | 1 sb =1cd cm$^{-2}$=10$^4$cd m$^{-2}$ |
| フォト | ph | 1 ph=1cd sr cm$^{-2}$ =10$^4$lx |
| ガル | Gal | 1 Gal =1cm s$^{-2}$=10$^{-2}$ms$^{-2}$ |
| マクスウエル | Mx | 1 Mx = 1G cm$^2$=10$^{-8}$Wb |
| ガウス | G | 1 G =1Mx cm$^{-2}$ =10$^{-4}$T |
| エルステッド(a) | Oe | 1 Oe ≙ (10$^3$/4π)A m$^{-1}$ |

(a) ３元系のCGS単位系とSIでは直接比較できないため、等号「 ≙ 」は対応関係を示すものである。

表10．SIに属さないその他の単位の例

| 名称 | 記号 | SI 単位で表される数値 |
|---|---|---|
| キュリー | Ci | 1 Ci=3.7×10$^{10}$Bq |
| レントゲン | R | 1 R = 2.58×10$^{-4}$C/kg |
| ラド | rad | 1 rad=1cGy=10$^{-2}$Gy |
| レム | rem | 1 rem=1 cSv=10$^{-2}$Sv |
| ガンマ | γ | 1 γ=1 nT=10$^{-9}$T |
| フェルミ | | 1 フェルミ=1 fm=10$^{-15}$m |
| メートル系カラット | | 1 メートル系カラット= 0.2 g = 2×10$^{-4}$kg |
| トル | Torr | 1 Torr = (101 325/760) Pa |
| 標準大気圧 | atm | 1 atm = 101 325 Pa |
| カロリー | cal | 1 cal=4.1858J（「15℃」カロリー），4.1868J（「IT」カロリー），4.184J（「熱化学」カロリー） |
| ミクロン | µ | 1 µ =1µm=10$^{-6}$m |

（第8版，2006年）